BU-DUMAND-94/1
February 18, 1994

DUMAND STAGE II STATUS REPORT *

Peter K. F. Grieder †
Department of Physics and Astronomy
University of Hawaii at Manoa
2505 Correa Road, Honolulu, HI 96822, U.S.A.

For the DUMAND Collaboration

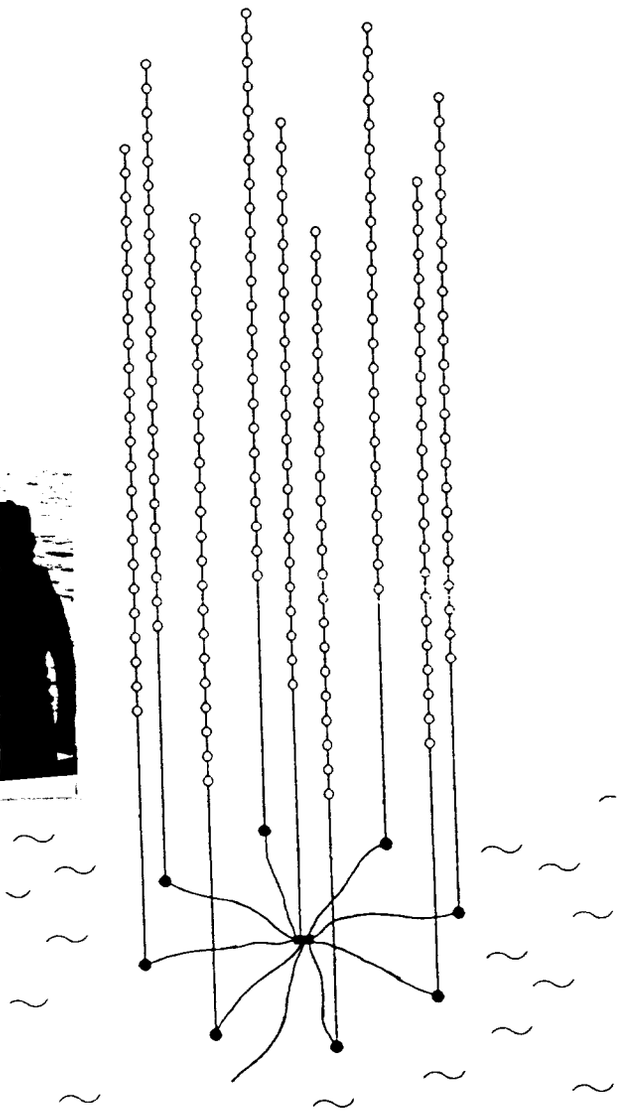

*Lecture presented at the 3rd Nestor Internat. Workshop, October 19 - 21, 1993, Pylos, Greece
†On leave from the Physikalische Institut, University of Bern, Switzerland

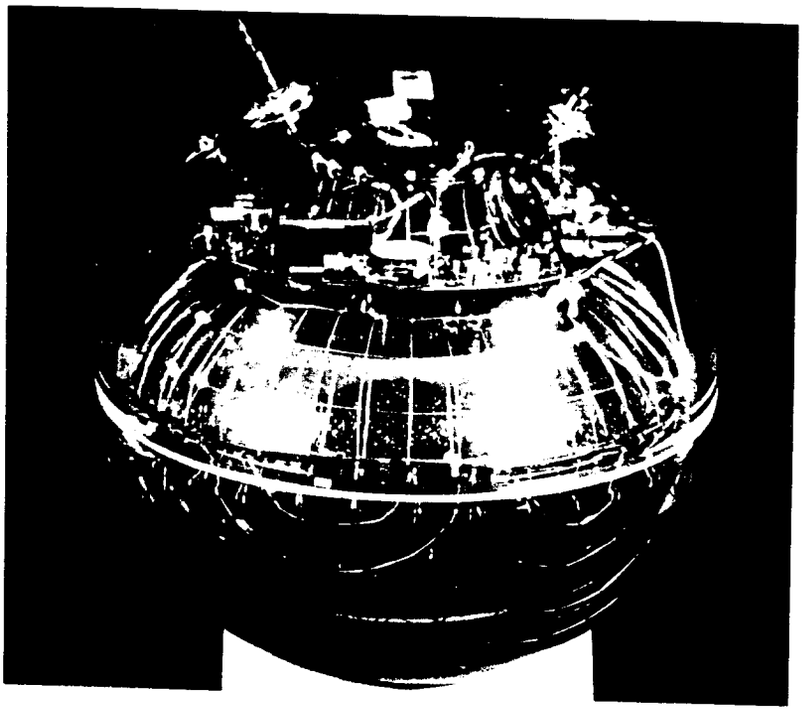

Above. Photograph of DUMAND optical Cherenkov detector module (JOM). The large 15" photomultiplier tube and the electronics board around its neck (pointing upward) are clearly visible through the ultraviolet transparent 17" Benthos glass sphere that serves as pressure housing. The two protruding objects near the center of the upper hemisphere are the electrical (left) and optical fiber (right) penetrators needed to power the module and access the data. On the lower left of the electrical penetrator is the vacuum port. The coarse wire mesh around the multiplier tube is the magnetic shield.

Cover Page:

Left. Deployment of DUMAND string 1, 30 km west of Keahole Point, Hawaii. An optical module is in the process of being lowered from the T. G. Thompson into the ocean (center right). On the left part of the junction box with the tapered bend relief and shore cable curving sharply downward is visible.

Right. DUMAND Stage II Octagon array. The small circles represent the optical detector modules, the full circles at the bottom the string anchors with the rectangular junction box in the center, and the shore cable.

BU-DUMAND-94/1
February 18, 1994

DUMAND STAGE II STATUS REPORT *

Peter K. F. Grieder †
Department of Physics and Astronomy
University of Hawaii at Manoa
2505 Correa Road, Honolulu, HI 96822, U.S.A.

For the DUMAND Collaboration *

Abstract

The DUMAND Stage II detector system, now under construction, is a giant three-dimensional array of 216 highly sophisticated optical Cherenkov detector modules, intended to be used as a muon and neutrino telescope. The system consists of nine so-called strings of 24 detector modules each; eight strings are located at the corners of an equilateral octagon, 40 m apart, with the ninth string at the center. The array's point source sensitivity is $4 \div 7 \cdot 10^{-10}\ \nu\ cm^{-2} s^{-1}$ per year above 1 TeV, its angular resolution $\approx 1°$. Phase I of this project, called the TRIAD detector, is now approaching completion. This phase includes deployment, installation and taking into operation of three out of the nine strings, and of a large multi-connector junction box in the center of the DUMAND site, at a depth of nearly 5000 m, approximately 30 km west of the most western tip of the island of Hawaii. It also includes laying the 12-fiber electro-optical cable from the junction box to shore, that powers the junction box and establishes multiple high-speed single mode command and data links between the deep ocean laboratory and the shore station. Various support systems such as a very high precision sonar, floodlights, television cameras, etc., are either integrated with or suspended above the junction box. These facilitate installation, recovery and re-installation after servicing of strings, and help to guide a robot or manned submersible when connecting equipment to the junction box. In the middle of December 1993, junction box, support systems and shore cable were successfully deployed and taken into operation. String 1 was simultaneously deployed and operated for about ten hours before a problem developed. It had since been recovered and is now being inspected. It will be re-install together with the two other strings in the near future. We briefly describe the system, summarize the project status and outline our future plans.

---

*Lecture presented at the 3rd Nestor Internat. Workshop, October 19 - 21, 1993, Pylos, Greece
†On leave from the Physikalische Institut, University of Bern, Switzerland
*For full list see end of paper

Contents

1 Introductory Comments

The DUMAND (DEEP UNDERWATER MUON AND NEUTRINO DETECTOR) project is a giant muon and neutrino telescope consisting of a 3-dimensional matrix of omnidirectionally sensitive optical Cherenkov detector modules in the deep ocean [1,2]. Late in 1987, after a long feasibility study and development period, the DUMAND collaboration has successfully completed the short prototype string experiment which paved the way for the construction of the first giant deep ocean muon and neutrino telescope [3].

At that time significant developments still lay ahead in electronics and optical communication systems, particularly in the fields of ultra high speed data handling and transmission where the technology was still inadequate to meet our demands. Moreover, construction and installation of a system of such complexity at a depth of nearly 5000 m in the ocean posed countless engineering, manufacturing and deployment problems of hitherto unknown magnitude.

These developments, many of which were joint ventures with the leading industries in the various fields, represented major technological challenges. Many of the vital components were either not available as off-the-shelf items or, if available, proved to be inadequate and necessitated custom design. Even today many components and subsystems that we use are cutting-edge technology and represent a first of their kind in the field.

In the following we will briefly review the scientific goals of DUMAND Stage II, system design, characteristics and capabilities, and highlight some of the more technical and operational aspects.

2 Scientific Goals of DUMAND

The scientific goals of the DUMAND project are basically fivefold [2]. They are listed below in order of priority.

1) High Energy Neutrino Astronomy and Astrophysics:
Search the universe for point and distributed sources of energetic muon and electron neutrinos and determine the gross features of the neutrino spectrum of these sources in an attempt to locate and study possible sources of cosmic rays and other astrophysical aspects [4]

2) Cosmic Ray Physics:
Study the properties of cosmic ray muons of energy $\geq$ 3 TeV , their production, propagation, interaction and spectral features as well as their multiplicity,

decoherence and lateral distribution, in order to deduce spectral features, chemical composition and other aspects of the parent primary radiation in the energy range between 10 TeV and 10^5 TeV [5].

3) Muon and Neutrino Physics:
Investigate neutrino interactions and other topics of particle physics at energies far beyond the range of present and planned accelerators. Study properties of neutrinos including neutrino oscillations at higher energies in hitherto untouched domains [6].

4) High Energy Gamma Ray Astronomy:
Search for ultra high energy gamma ray point sources via TeV muon astronomy, provided that less conventional muon production processes do indeed play a significant role.

5) Miscellaneous Topics:
The DUMAND array is optimized for the tasks and in the order of priority listed above. However, related topics such as supernova watch, the search for particular forms of dark matter, and others will be pursued along as sidelines.

It is also evident that DUMAND and its support systems make it possible to carry out a wide variety of research projects in other fields. As an example, the optical detector matrix in combination with the highly sophisticated DUMAND sonar system permit the energy calibration of acoustic shocks produced by large cascades in the ocean within and around the array. Subsequently acoustic shocks produced by ultra high energy events at large distances from the array can be used as a tool to explore the primary cosmic ray spectrum from the ankle ($\geq$ 10^{19} eV) to the highest energies, to search for a cut-off [7].

In addition long-duration measurements and experiments in the fields of oceanography, marine biology, geophysics, environmental sciences and climatology are well within the range of capabilities of the DUMAND deep ocean laboratory. Further details of the scientific program are given in the DUMAND proposal [2].

3 The DUMAND Stage II Detector

3.1 Array Layout.

The layout of the detector matrix is illustrated in Fig. 1. The array consists of 9 strings with 24 optical Cherenkov detector modules each, totalling 216 detector modules. The modules on a string have a vertical separation of 10 m with the first module located 100 m above the sea floor to avoid possible optical background from near bottom dust clouds or dirt sedimentation on the lower modules after impact

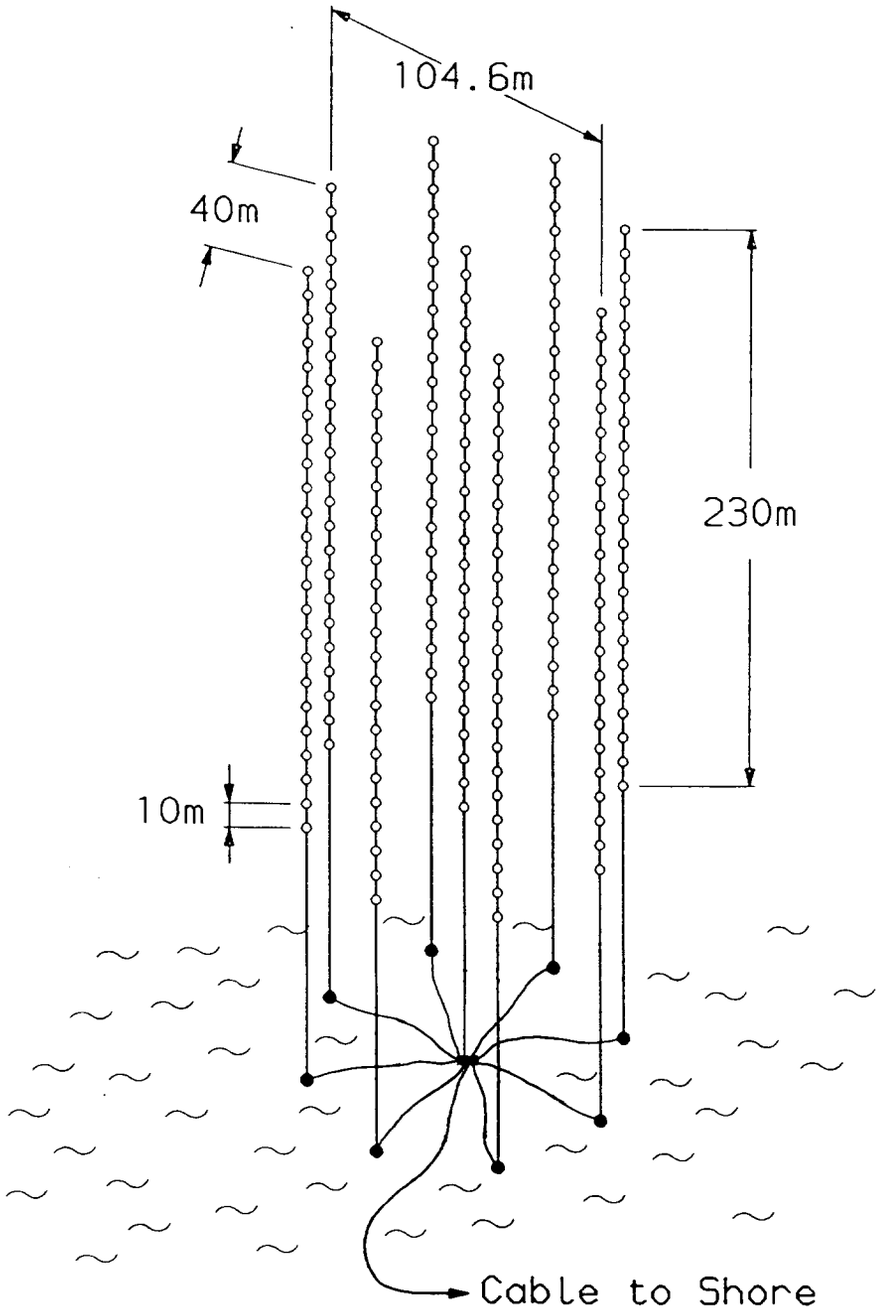

Figure 1: DUMAND Stage II Octagon array layout with its nine strings of 24 optical Cherenkov detector modules each, totalling 216 modules. Each string is connected to the central junction box which is linked to the shore station via a 12-fiber electro-optical cable that supplies power and handles high-speed bi-directional communication.

of the string anchor on the ground [1]. The strings are located 40 m apart on the corners of an octagon with the ninth string at its center. The octagon measures 105 m across. The overall height of a string is 425 m, measured from the anchor to the top floatation unit. Further details are given in Table 3.1.

Within the given budget, the principal design parameters of the muon and neutrino telescope, such as matrix size, configuration, module and string spacings were, determined chiefly by the scientific objectives of the experiment, the optical attenuation length of the water at the site, and to some extent by the characteristics of the detector modules [8]. Furthermore, extensive site surveys including water transparency and current measurements [9], background light measurements [10,11], the performance of the prototype string experiment and its results [3] offered additional guidelines for the design.

In principle, such a detector system is almost freely expandable to any size as may be required to meet specific scientific objectives. Due to the fact that the DUMAND site is located at great depth in the ocean it can employ the water masses of the ocean simultaneously and very effectively as a multipurpose medium for the following tasks:

-As an excellent shield against the unwanted cosmic ray background,
-as a well behaved homogeneous absorber of particles and radiation without imposing topographical problems,
-as target for muon and neutrino interactions,
-as Cherenkov radiator for charged particles,
-as dark room to prevent daylight from interfering with the faint Cherenkov light, and
-as high energy acoustic shock generation target and propagation medium.

3.2 Site and Infrastructure.

The DUMAND site is located about 30 km west of Keahole Point on the island of Hawaii (the Big Island), approximately 250 km southeast of Honolulu, which is on the island of Oahu (Fig. 2). The ocean floor at this location is 4750 m below sea level and consists of a vast and almost perfectly flat dessert-link plane of silt that extends miles in all directions. To the east of the site's center, some 5 km away, begins the steep and jagged ridge with deep trenches and canyons which consists of old lava flows that rise to the rugged shore line of Kona. Fig. 3 shows an artist's conception

[1]Several inspections of the sea floor carried out with a video camera at the DUMAND site have revealed that the area is essentially dessert-like and practically uninhabited by fish or crawling animals. Objects that are being lowered impact slowly, causing only small clouds of silt that extend but a few feet above the ground and are readily swept away by the slight current.

TABLE 3.1 : Summary of Major Array and Site Characteristics.

Longitude of array center	156.325° W
Latitude of array center	19.725° N
Depth of ocean floor	4750 m
Array dimensions	105 m diameter, 230 m high
String spacing	40 m side, 52.5 m to center
Number of strings in array	8 on contour, 1 in center
Sensor spacing along string	10 m
Number of optical sensors/string	24
Total number of optical sensors	$9 \cdot 24 = 216$
Height of first sensor	100 m above sea floor
Sensor pressure envelope	17" (43.2 cm) O.D., glass
Optical sensor	15" photomultiplier
Volume of array, contained	$1.8 \cdot 10^6$ m^3
Target area for through-going muons	23,000 m^2 horizontal 7,850 m^2 vertical up-going 2,500 m^2 down-going
Area-solid angle product for neutrino induced muons	148,000 $m^2 sr$
Effective target volume for 2 TeV muons	$1.0 \cdot 10^8$ m^3
Effective target volume for 1 TeV cascades	$7.0 \cdot 10^5$ m^3
Muon energy threshold	$20 \div 50$ GeV
Track reconstruction accuracy	$0.5° \div 1.0°$
Cascade detection threshold	$\approx$ 1 TeV
Muon rate, down-going	3 per minute
Atmospheric neutrino detection rate for through-going muons	3500 per year
Atmospheric neutrino detection rate for contained events > 1 TeV	50 per year
Point source sensitivity	$4 \div 7 \cdot 10^{-10}$ $cm^{-2} s^{-1}$ per year above 1TeV
Contained event sensitivity	10^{-8} cm^{-2} s^{-1} per year above 1 TeV

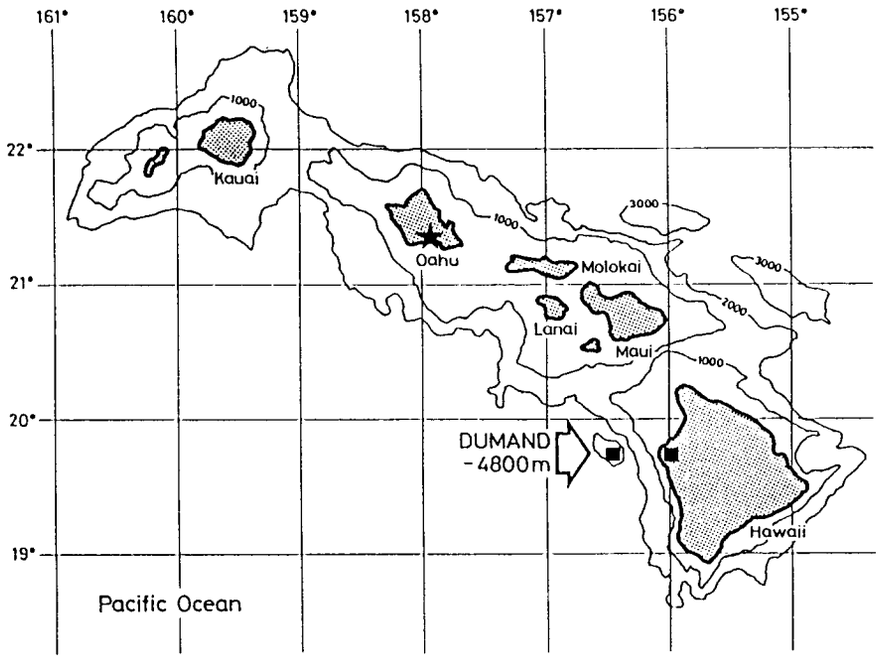

Figure 2: Map of the Hawaiian islands. The DUMAND site and shore station are indicated by the black squares at the lower right, Honolulu by the star on the island of Oahu, about 250 km north west of the site.

of the site with the array implanted and the shore facilities. The site is fairly well protected from the strong Mid-Pacific ocean currents that pass between the islands and is partially shielded from the Tradewinds by the Big Island's mountain ranges, that reach heights of 4000 m a.s.l..

At the bottom of the array, a large junction box (Fig. 4) offers the basic infrastructure such as electric power and multiple high performance two-way communication links for system control and data acquisition.

Autonomous battery powered transponders with their geographic coordinates precisely known and the capability to remain operational for about five years, are distributed along a circle of radius 1.5 km, centered at the site. Additional sonar responders that will be deployed at a later time and connected to the junction box by a robot are positioned at closer proximity to the site's center. They are part of a highly sophisticated sonar system that employes a new technique which makes it possible to locate the position of each Cherenkov detector module in the DUMAND array within a geographically fixed frame of reference, with origin centered at the junction box, to an accuracy of a few centimeters. After deployment the absolute geographic position of the junction box can be determined to an accuracy of two meters.

Two video cameras coupled with searchlights that can be rotated around two axes each (tilt and pan) are mounted 10 m above the junction box. They permit

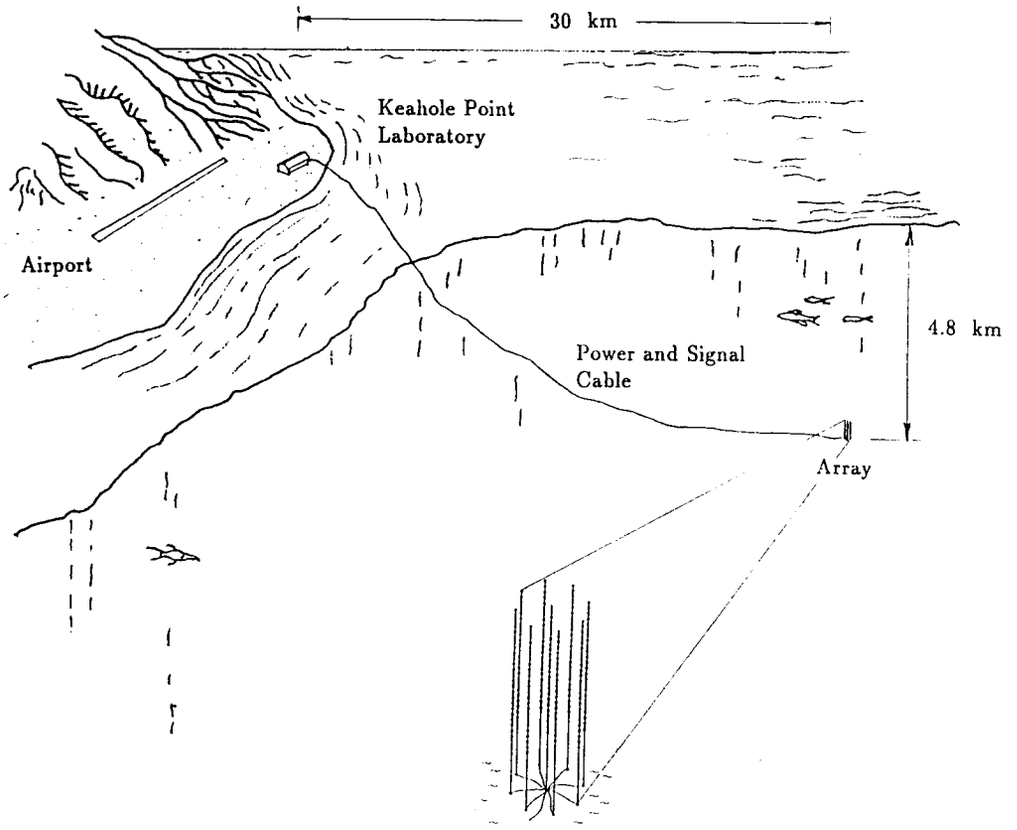

Figure 3: Artists' conception of the array moored on the ocean floor with the Keahole Point laboratory and airport 30 km to the east on the Big Island.

to observe deployment and installation of the junction box and offer valuable assistance when installing, recovering or exchanging strings during the initial or later deployment operations, and to inspect the junction box in the future. The video and part of the sonar system are mechanically part of string 1, which is directly connected to the junction box. However, these units represent an independent system with its own command and data link to shore. It should be regarded as part of the infrastructure of the deep ocean laboratory and not as part of string 1 since the standard string portion can be released and recovered (or re-installed) while video and sonar systems remain operational.

The shore station is located at the Hawaii Natural Energy Laboratory at Keahole Point, about 10 miles north of Kailua Kona, on the Big Island. A 200 m long cable conduit is provided to take the twelve-fiber electro-optical cable from the laboratory building directly into the ocean 10 meters below the water line to prevent the cable from being damaged by the surf.

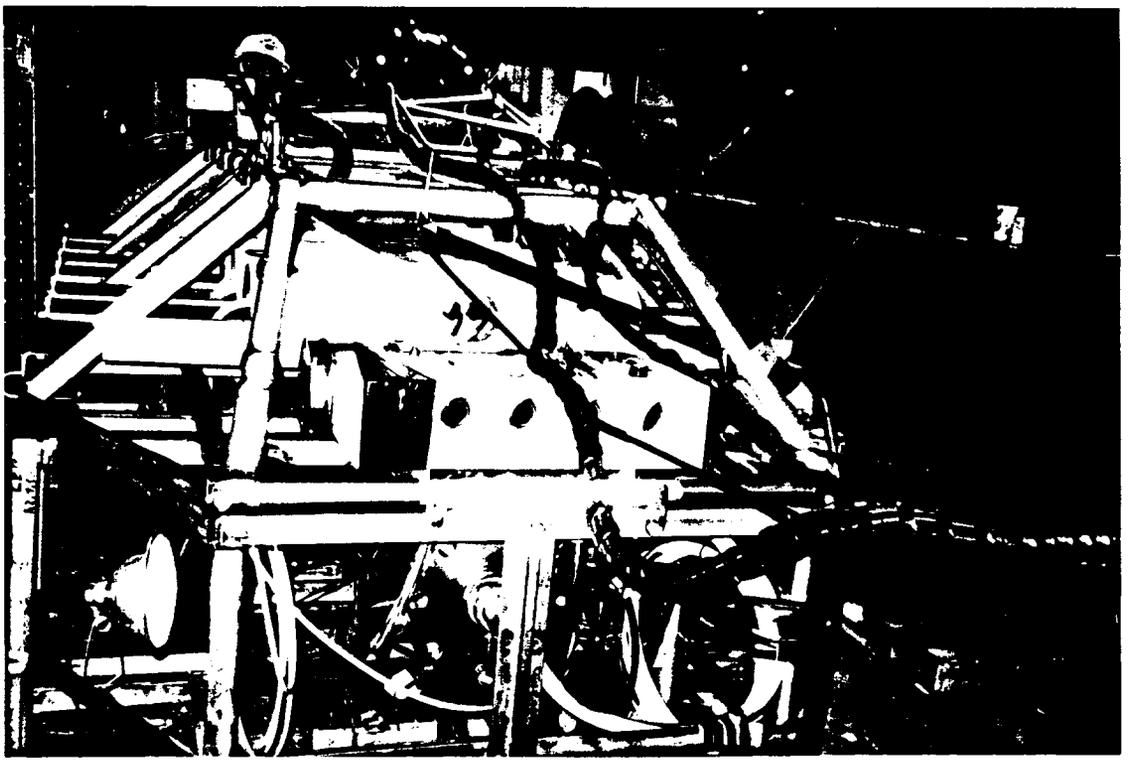

Figure 4: Photograph of titanium junction box with six wet matable connectors on either side shortly before deployment. Each connector supplies fused 350 V dc and a single mode optical fiber link to shore. The fibers are suitable for simultaneous bi-directional communication on 1550 nm and 1300 nm. In addition the junction box houses the control and communication system for the high precision sonar and video systems, and has provisions to connect sonar responders to be deployed later by a robot.

3.3 String Configuration and Details.

Each DUMAND string is a fully independent subsystem that can be placed separately on the sea floor and connected subsequently to the junction box by a remotely operated robot or a manned deep sea submersible. Either option had been tested successfully with a dummy junction box on the sea floor at the site in November 1992, using our custom designed wet matable connectors. Once lowered to the sea floor at some distance from the junction box, a wide variety of experiments can be powered and operated from shore via shore cable and junction box.

The configuration of a typical string is shown in Fig. 5. Besides the 24 optical detector modules, which are briefly described below, each string is equipped with two (in some cases three) optical calibration modules. These consist of nitrogen laser activated scintillation spheres which emit very short isotropic light flashes upon command. These allow periodic monitoring of the detector performance, such as

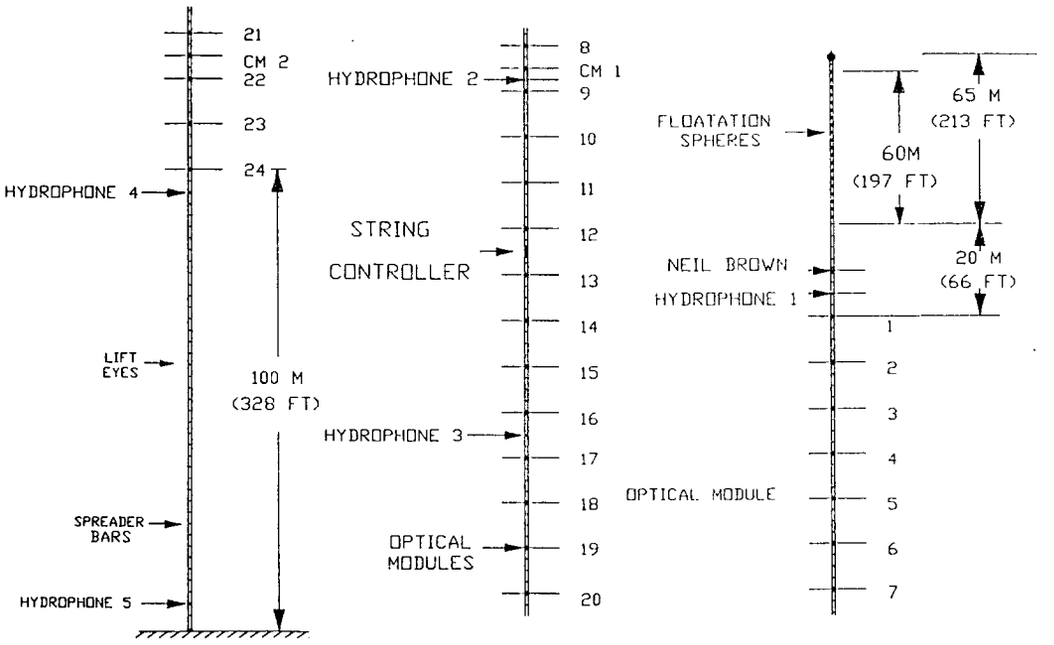

Figure 5: Detailed layout of the central string showing the location of the optical Cherenkov detector modules, the laser activated calibration modules, hydrophones, Neil Brown environmental module, floatation units, and the flasher and radio beacon at the top.

timing and sensitivity, enabling us to re-calibrate each module individually and to carry out optical attenuation length measurements in the water.

Five wide-band hydrophones are distributed along each string. They serve two purposes. Firstly, in conjunction with our sophisticated sonar system, mentioned above, they permit to track and determine the location of the modules continuously and to a high degree of accuracy [12]. This guarantees maintenance of the high angular resolution and absolute pointing accuracy of the telescope at all times.

Secondly, the acoustic array formed by the hydrophones will be used in conjunction with the Cherenkov array in a feasibility study with the aim to correlate acoustic shocks, initiated by ultra-high energy cosmic ray events in the ocean, with the energy of the events, as discussed earlier. If successful, this method would open the possibility of exploring the upper end of the cosmic ray spectrum with huge acoustic arrays, much larger than any presently planned air shower array, at a fraction of their cost [7].

Each string is also equipped with an environmental module which has a compass for orientation and measures ocean currents in two directions, string acceleration in three directions, ocean temperature and salinity. The strings are optically identical

with respect to the Cherenkov detector modules[2] but differ slightly in the number of calibration modules. Even numbered strings on the circumference of the octagon and odd numbered strings are equipped alike, respectively. The center string which rises directly from the junction box differs from all the others insofar as the lower portion of the tare height which is kept blank on all other strings, holds additional equipment (floodlights, TV cameras, sonar devices), as mentioned above. To optimize array timing the center string has two European optical modules. These have a faster pulse rise time than the Japanese modules for reasons explained elsewhere [13].

The upper most 60 meters of each string hold a number of floatation units to give the string the necessary buoyancy. At the very top is a unit which houses a radio beacon and flashers that are activated when a string reaches the surface, after being released acoustically from its anchor, to facilitate recovery at sea.

An integral part of each string is the string controller which is located at the center of the string, between modules number 12 and 13, for timing reasons. The data from all the modules on a string (incl. optical, calibration, and environmental modules, as well as the hydrophones) are converted to semi-analog optical signals inside the modules and transmitted via multi-mode optical fibers to the string controller. There the signals are digitized, time stamped, labelled and converted to 40 bit words. The latter are injected at a rate of 500 Mbd (later on 1 Gbd) by a laser at a wavelength of 1550 nm into a single mode fiber, and sent via junction box and cable to the trigger processor and data acquisition system on shore.

The string controller is powered directly from the junction box, converts the voltage, and powers the various modules. Each module power line is at the same time a 300 baud two-way command and data link that allows to control and monitor all relevant module parameters from shore. They also allow to download new programs to the modules' processors and memories. The commands from shore to a string are sent on the same single mode fiber that carries the high speed data from the string to shore, but in a different color (1350 nm). The commands for the different modules are de-multiplexed in the string controller which performs a large number of additional tasks as well.

3.4 System Capabilities and Background.

The geographic location of DUMAND, close to the equator (19.725° N and 156.325° W), combined with the great depth of the detector matrix of almost 5000 m make DUMAND a very unique neutrino telescope.

Unlike other, more shallow detectors, that are confined to a relatively small solid

[2]There are slight differences between the Japanese and European versions of the optical modules that are discussed in the technical section.

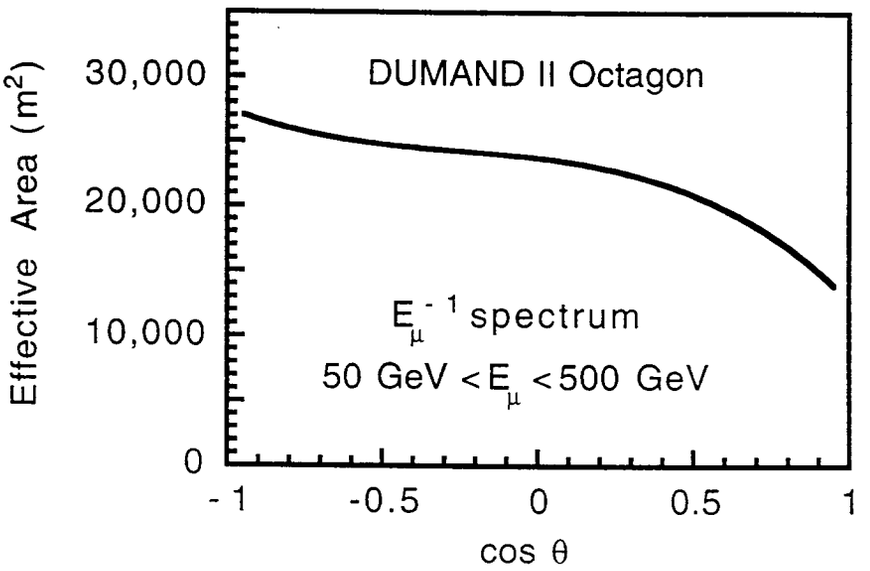

Figure 6: Effective area of the DUMAND II Octagon array versus cosine of zenith angle θ, for muons of energy between 50 GeV and 500 GeV. The simulation is based on a power law energy spectrum for the muons of integral form E_μ^{-1}.

angle field of view, centered about the downward direction, DUMAND can view the sky not only over the entire lower hemisphere but well above the horizon, to a zenith angle of about 75°, without being seriously impaired by cosmic ray muons of atmospheric origin, faking neutrino induced muons, that add to a problematic background. In fact, DUMAND can observe 2.35 steradian of the universe simultaneously. Moreover, it can perform essentially a complete scan of the entire universe every day, whereas detectors located at the Earth's poles are restricted to view the same small solid angle of the sky at all times.

The DUMAND detector modules manifest omnidirectional optical sensitivity, however, the sensitivity is not isotropic. Therefore the modules in the array are oriented with their peak sensitivity facing downward, to optimize the detection probability for upward directed muons, originating exclusively from neutrino induced interactions. Nevertheless, the array can be also used for downward going muons. Fig. 6 shows the effective area of the DUMAND II Octagon as a function of the cosine of the zenith angle, θ, for muons covering the energy range 50 GeV $\leq E_\mu \leq$ 500 GeV, and Fig. 7 shows the averaged area as a function of muon energy. The array is also sensitive to larger hadronic and electromagnetic cascades. Additional array characteristics are given in Table 3.1.

The array response to atmospheric neutrino initiated events is presented in Fig. 8. Shown is the differential atmospheric neutrino spectrum on an arbitrary scale (dashed curve) and the number of reconstructed muon tracks versus neutrino

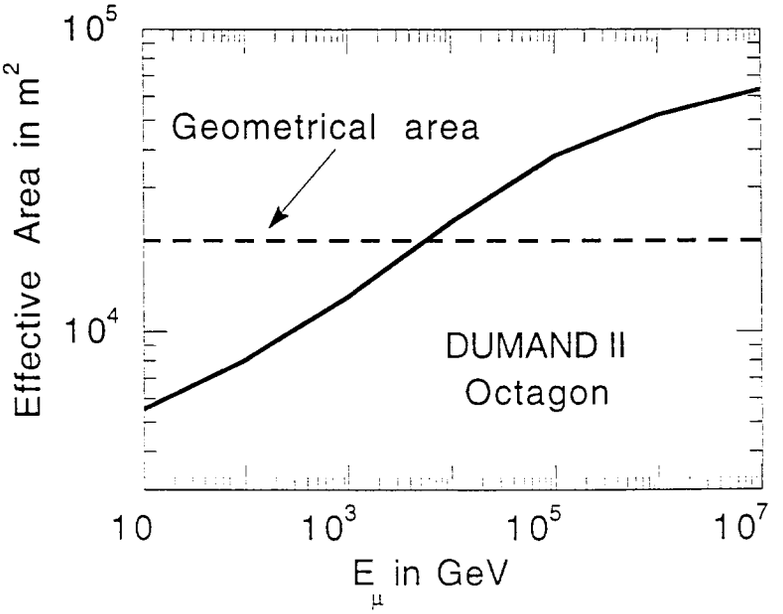

Figure 7: Average effective area of the DUMAND II Octagon array versus muon energy. The dashed line indicates the averaged geometrical area.

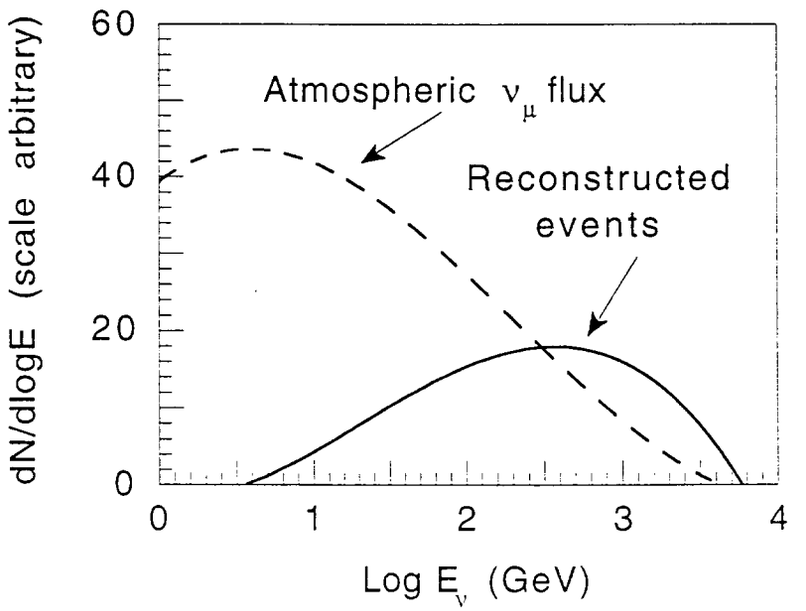

Figure 8: Number of fully reconstructed muon trajectories versus neutrino energy for an atmospheric neutrino spectrum of the form shown by the dashed curve.

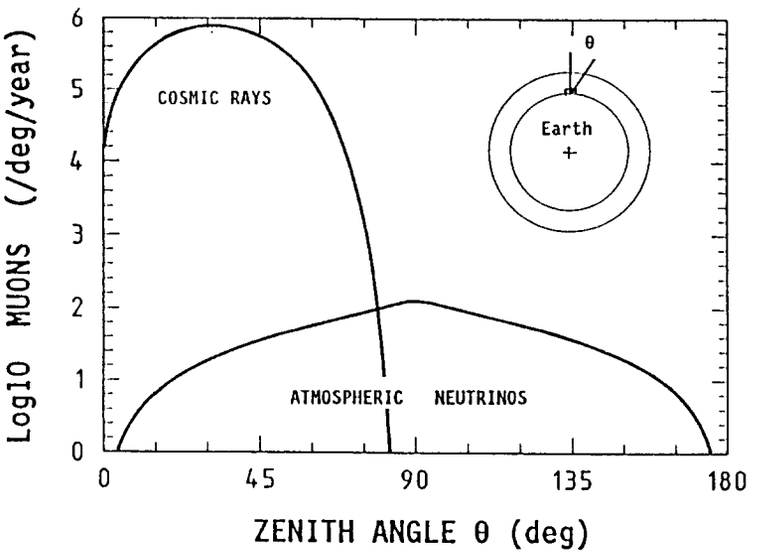

Figure 9: Calculated distribution of through-going muons in the DUMAND Stage II array from cosmic rays and atmospheric neutrino events, as a function of the muon zenith angle, θ.

energy (solid curve). This second curve shows how the track reconstruction efficiency rises with increasing neutrino energy because of the increasing muon energy and track length. The expected zenith angle distribution of through-going muons in the DUMAND Stage II array originating from cosmic rays and atmospheric neutrino events, respectively, is shown in Fig. 9.

The most probable angular resolution of the array is 0.8° [14]. High angular resolution reduces the background per pixel (approx. $0.017^2\pi$ sr) and, thus, improves the detection sensitivity for extraterrestrial neutrino sources. The background counting rate per pixel is approximately 1.5 events per year. The contributions from the different sources that are responsible for the background are given in Table 3.2. Cherenkov light from K^{40} radioactivity contributes significantly to the background, more than the occasionally large but short bioluminescence outbreaks that last typically about one minute [10,11].

The minimum detectable flux for a background of one event per year per pixel and an effective detector area of 20.000 m^2 for a neutrino differential energy spectrum of the form $dF_\nu/dE \propto E^{-2}$ is $1.2{\cdot}10^{-10}$ $cm^{-2}s^{-1}$ at $E_\nu \geq 1$ TeV. This flux yields 10 events per year per pixel [15]. [t] shows the energy dependence of the average value of α.

The octagon will not be able to say much about the energy of individual muons. However, because of its large size, the array will be able to record occasional short bursts of high light levels along the trajectory of very energetic muons that are due to cascades from muon bremsstrahlung or nuclear scattering. In Fig. 10 we show the

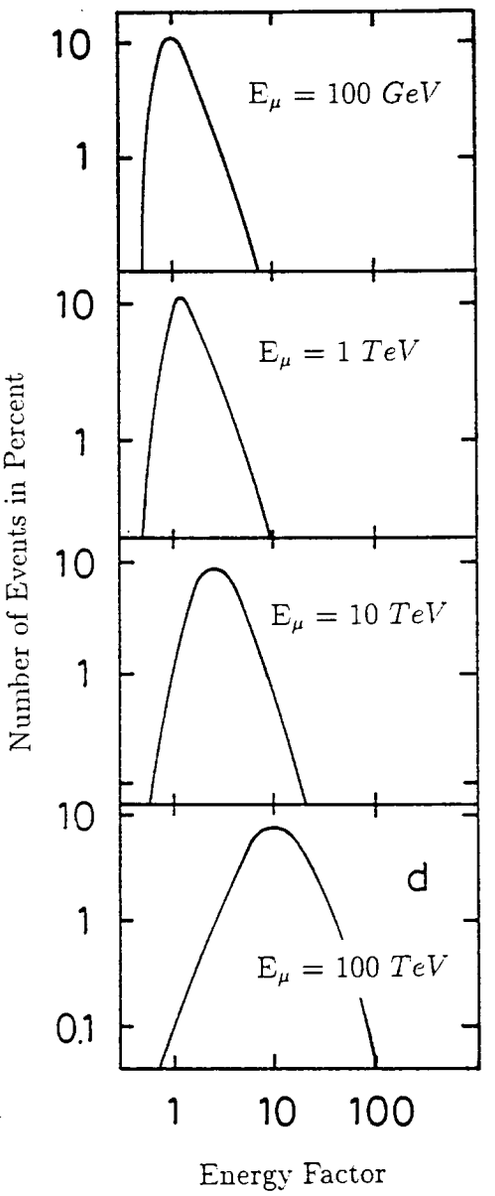

Figure 10: Distribution of the percentage of events as a function of the energy factor as defined in the text for muons of different energy groups.

TABLE 3.2 : Background Sources and Counting Rates in DUMAND II.

Source	y^{-1} $(1^{\circ\,2}$ pix$)^{-1}$
K^{40}	0.40 ± 0.08
Cosmic ray muons	0.63 ± 0.36
Cosmic ray multi-muons	0.15 ± 0.07
Atmospheric neutrinos	0.13 ± 0.01
Total	1.31 ± 0.38
Enclosed volume	$2 \cdot 10^6$ m^3

distribution of a so-called *energy factor* [3], α, for muons of different energy, ranging from 100 GeV to 100 TeV, and Fig. 11

Simulations indicate that sufficient information can be obtained so as to make a cut that will allow to separate statistically muon tracks originating from atmospheric neutrinos, which have a much steeper spectrum, from those initiated by high energy extraterrestrial neutrinos exhibiting a much flatter spectrum. This is illustrated in Fig. 12 for a Stecker type spectrum [16] of neutrinos from active galactic nuclei (AGN), as shown in Fig. 13, with an intensity reduced by a factor of 30, in comparison to the atmospheric neutrino spectrum [17]. With an adequate number of events it should be possible to determine the spectral index of a source.

If active galactic nuclei emit ultrahigh energy (PeV) neutrinos, as predicted theoretically, the DUMAND II array will have some sensitivity for detecting single, isolated cascades produced outside the array by ultrahigh energy muons from muon neutrinos of either kind and by electron neutrinos. In the first case the dominating contribution to the Cherenkov flash will be from the cascade and not the muon, in the latter it will be the cascade only. Preliminary simulation results indicate that the median angular error for 5000 TeV events would be 3.6° if the events occur at a distance of $\leq$200 m from the array center, and 12.3° if the distance is between 200 and 300 m [18]. The estimated counting rate for *all* AGN neutrino initiated events per cosine zenith angle interval, using a Biermann type spectrum [19] (see Fig. 13),

[3]The energy factor is essentially the ratio of measured light to that expected for minimum ionization.

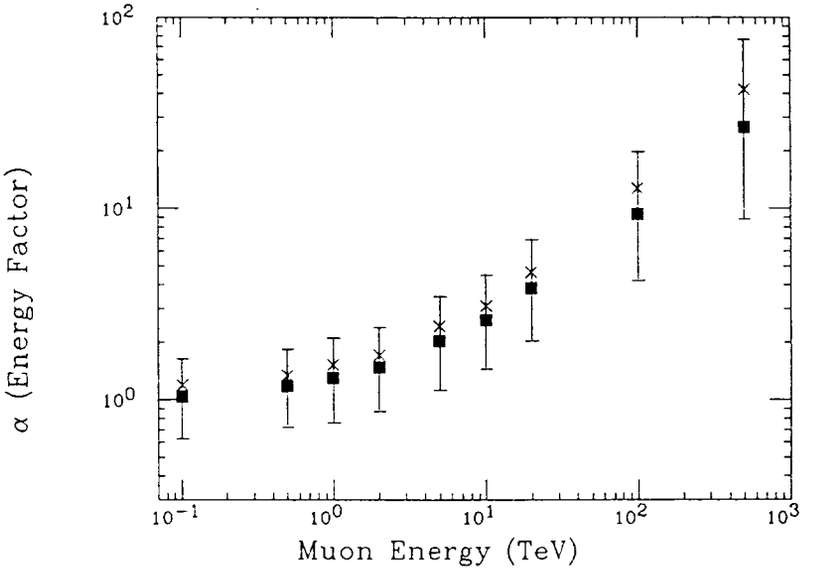

Figure 11: Dependence of the energy factor, α, on muon energy.

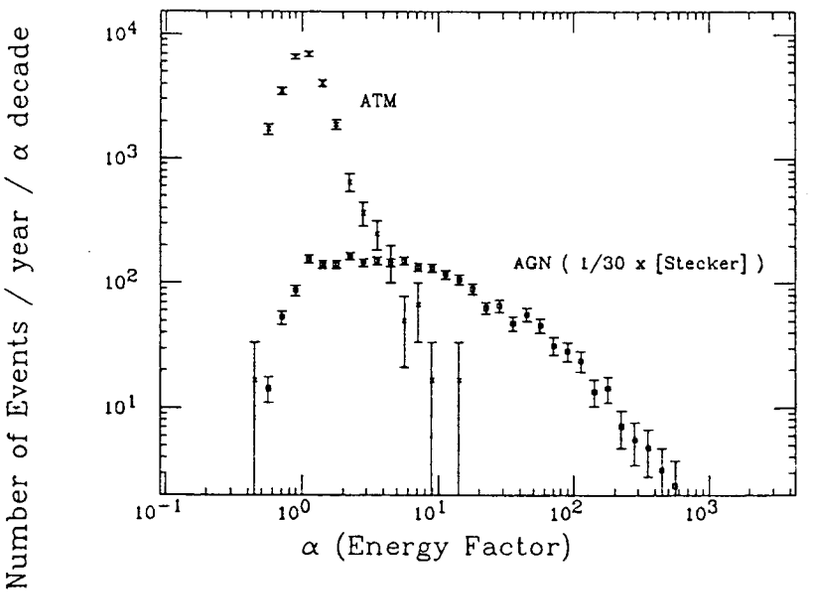

Figure 12: Distinction between atmospheric and very high energy extraterrestrial neutrinos from active galactic nuclei. The spectrum of the latter is based on the Stecker model, reduced in intensity by a factor of 30.

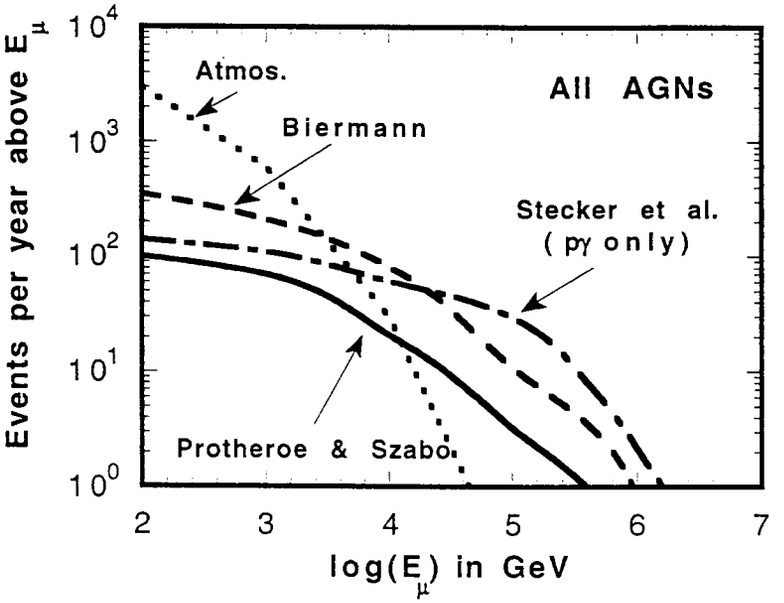

Figure 13: Atmospheric and extraterrestrial neutrino initiated events per year in DUMAND II as a function of muon energy. The different AGN neutrino initiated muon spectra apply to different AGN models, as indicated.

is shown in Fig. 14 together with the expected atmospheric neutrino events for two different energy regions [15].

The array's capability to search for neutrino oscillations is discussed elsewhere [20]. We present here only the result of these calculations in Fig. 15, showing the regions that DUMAND II could investigate.

4 Operating Principle and Technical Aspects

In many ways DUMAND is a pioneering experiment. Apart from being the first giant deep ocean neutrino telescope, it also employes cutting edge technologies in many fields such as electronics, ultra high speed data handling and processing, fiber optic communications, deep ocean engineering, sonar systems, and many more. In the following we will outline the operating mode of the experiment, including command and data handling and transmission, and briefly describe the optical Cherenkov detector module.

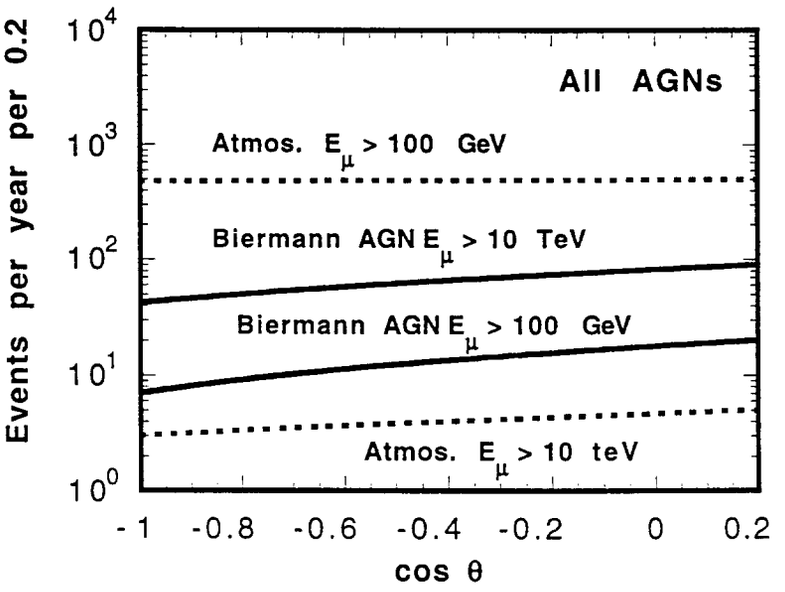

Figure 14: The zenith angle distribution of AGN neutrino events in DUMAND II, compared to the atmospheric background, for two cuts in muon energy. The Biermann neutrino flux is used for illustration.

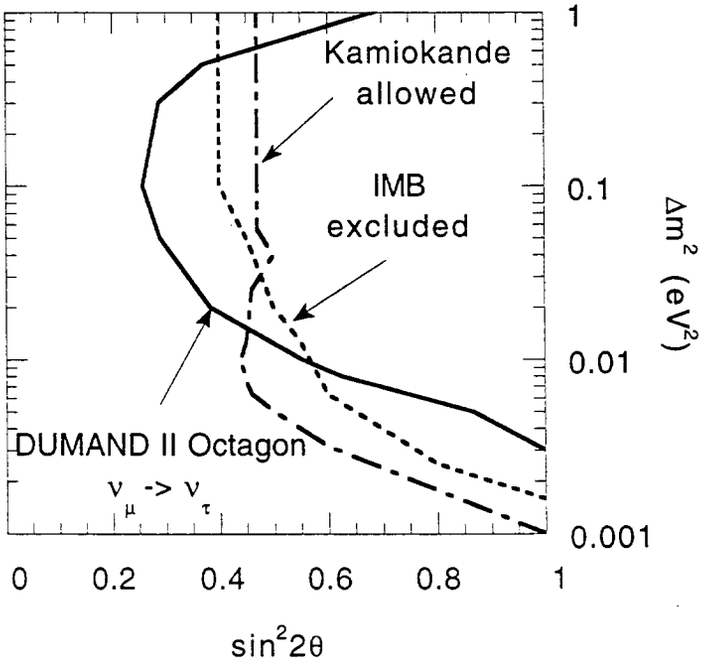

Figure 15: The range of oscillation parameters accessible to DUMAND II. Shown are the regions allowed by Kamiokande and excluded by IMB.

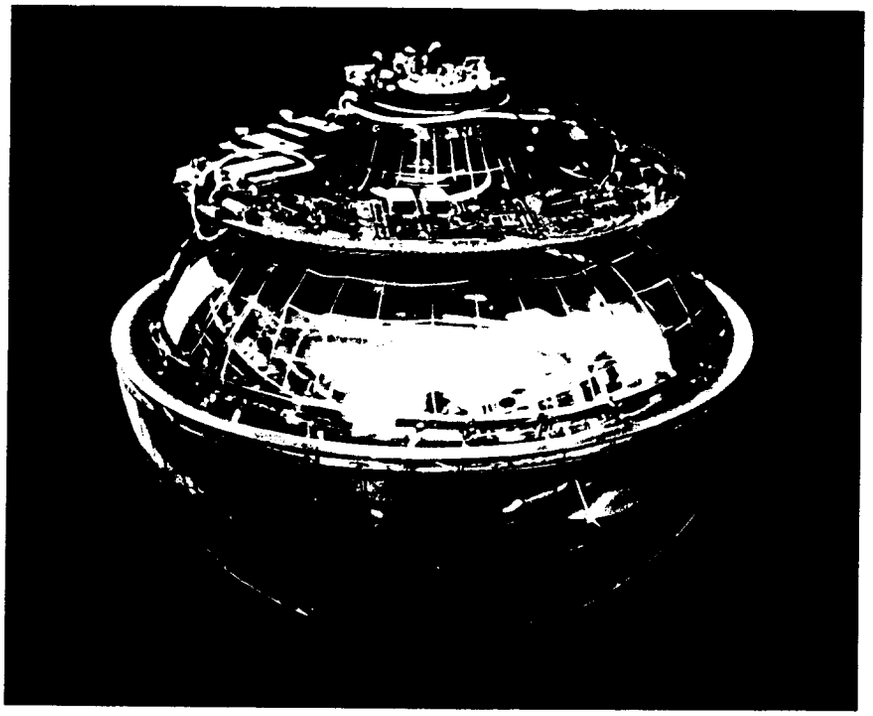

Figure 16: Photograph of DUMAND Cherenkov detector module with upper hemisphere of glass pressure housing removed. The 7-layer printed circuit board holds power converters, PMT high voltage supply, processor with memory, discriminator and electro-optical signal converter to send the data via optical fiber to the string controller. The wire mesh over the large photomultiplier tube is the magnetic shield.

4.1 Optical Modules

DUMAND uses two kinds of optical modules, the Japanese module [21,22] and the European module [23]. The two modules are essentially identical in their function and fully interchangeable within the array. Fig. 16 is an outline drawing of the Japanese module. A 15 inch Hamamatsu photomultiplier tube (PMT) is used in the Japanese module, whereas the European module uses the "Smart" 15 inch tube from Philips. The Japanese module generates for each detected signal a fast rising pulse that is proportional in duration to the time the PMT pulse remains over a prefixed discriminator threshold, i. e., the pulse length is proportional to the logarithm of the pulse height.

In addition, if the signal exceeds a prefixed level it also generates a second pulse whose length is proportional to the logarithm of the total integrated charge produced by the pulse at the anode of the PMT. The Philips tube has a somewhat faster rise time but not a monotonously falling exponential output pulse. Consequently time over threshold is not a good logarithmic measure of pulse height for the European module, and integrated charge only is used together with the fast leading edge of

the pulse for timing, as in the case of the Japanese module. In either case the pulses are converted to infrared optical pulses and transmitted from the modules via multimode optical fibers to the string controller in the center of the string.

4.2 Data and Command Flow

The data transmitted by the modules in the form of infrared light pulses on the fibers linking the modules with the string controller are converted to electrical pulses and digitized with a resolution of 1 nanosecond. For each event a 40 bit word is formed which includes module address and real time from a local clock. The time-stamp is corrected after each roll-over with respect to the shore standard. Digitization of the data from all 24 modules, the 5 hydrophones, and the environmental and calibration modules is done in a single GaAs chip, as shown in Fig. 17. The digitizer chip is a custom design made by the collaboration in a joint venture with industry [24]. It is at present one of the most advanced and fastest chips of its kind, holding nearly one million active elements.

The parallel data are placed into a buffer from where they are transferred at a constant rate to a serializer and laser driver. Subsequently a laser transmits the data at 500 MHz and a wavelength of 1550 nm via wavelength division multiplexer and single mode fiber to shore. There the data pass another wavelength division multiplexer and are converted by a receiver from optical to electrical pulses. The serialized data are again converted to 40 bit parallel data and split into different data channels, as indicated in Fig. 18

Each module is powered by 48 volts and controlled by a 68301 processor with its own resident program that supervises module operation and performs housekeeping functions and handles the dialogue with the shore station. The 48 volt power lines are also used for two-way communication with the modules. A modem in each module establishes the dialogue link with the string controller, and two separate computers in the latter extend the link via digitizer to shore.

The command link from shore is also indicated in Fig. 17 and Fig. 18. The commands or data needed to operate the system are sent from terminals on the shore or from any of the collaborating laboratories that is on duty at the particular time to a computer at the shore station. From there a laser, transmitting at 1300 nm, sends the commands or data via wavelength division multiplexer and single mode fiber to the string controller. There the two dedicated computers re-transmit the commands or data to the appropriate module.

Thus, complete control over the entire system including not only the modules, but also the string controller can be exercised from shore. This includes from individual adjustment and monitoring of all relevant parameters and levels in each module separately to downloading of a new module operating program. OS-9 is used to

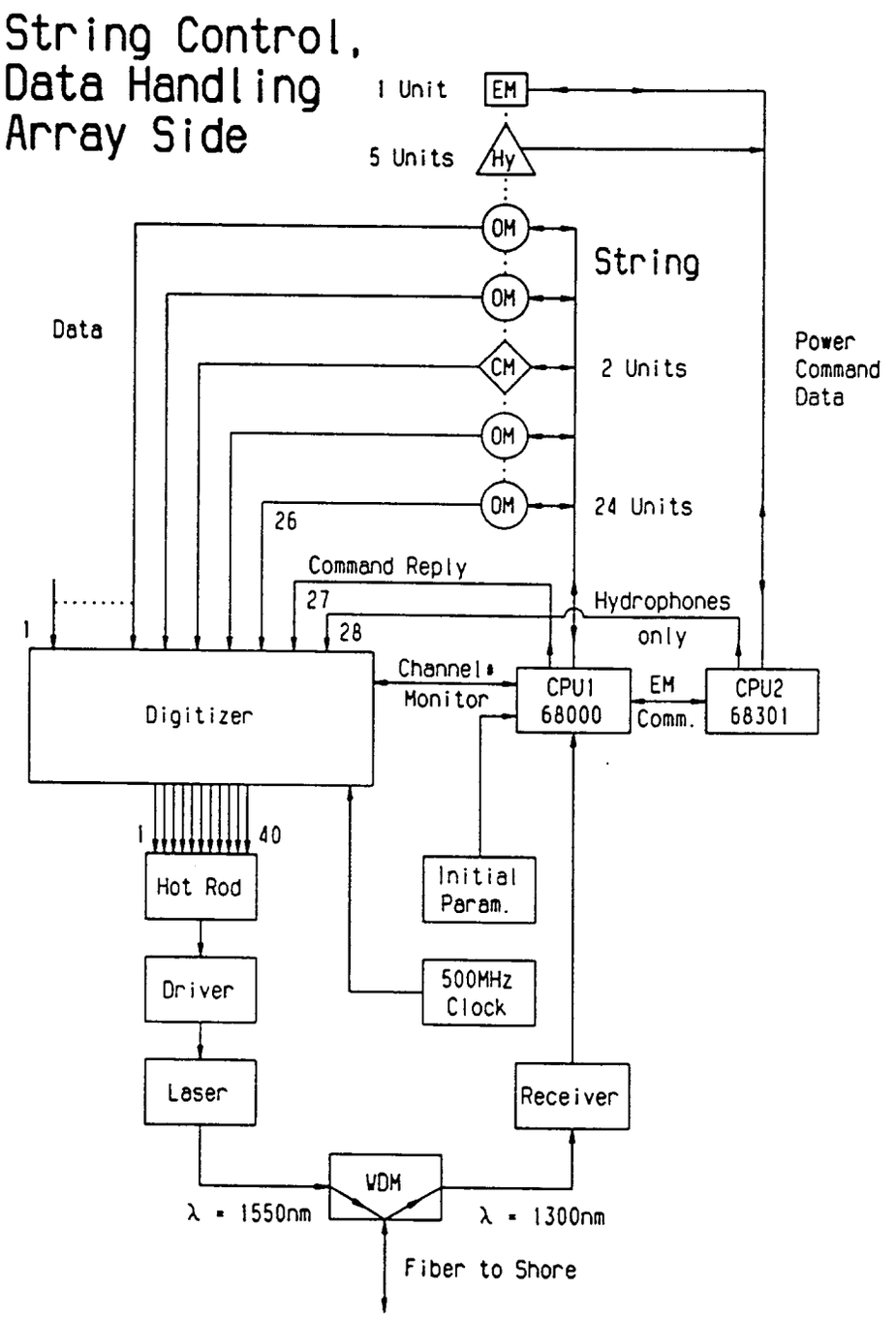

Figure 17: Block diagram of control and data flow of a string at the array side, in the ocean. For details see text.

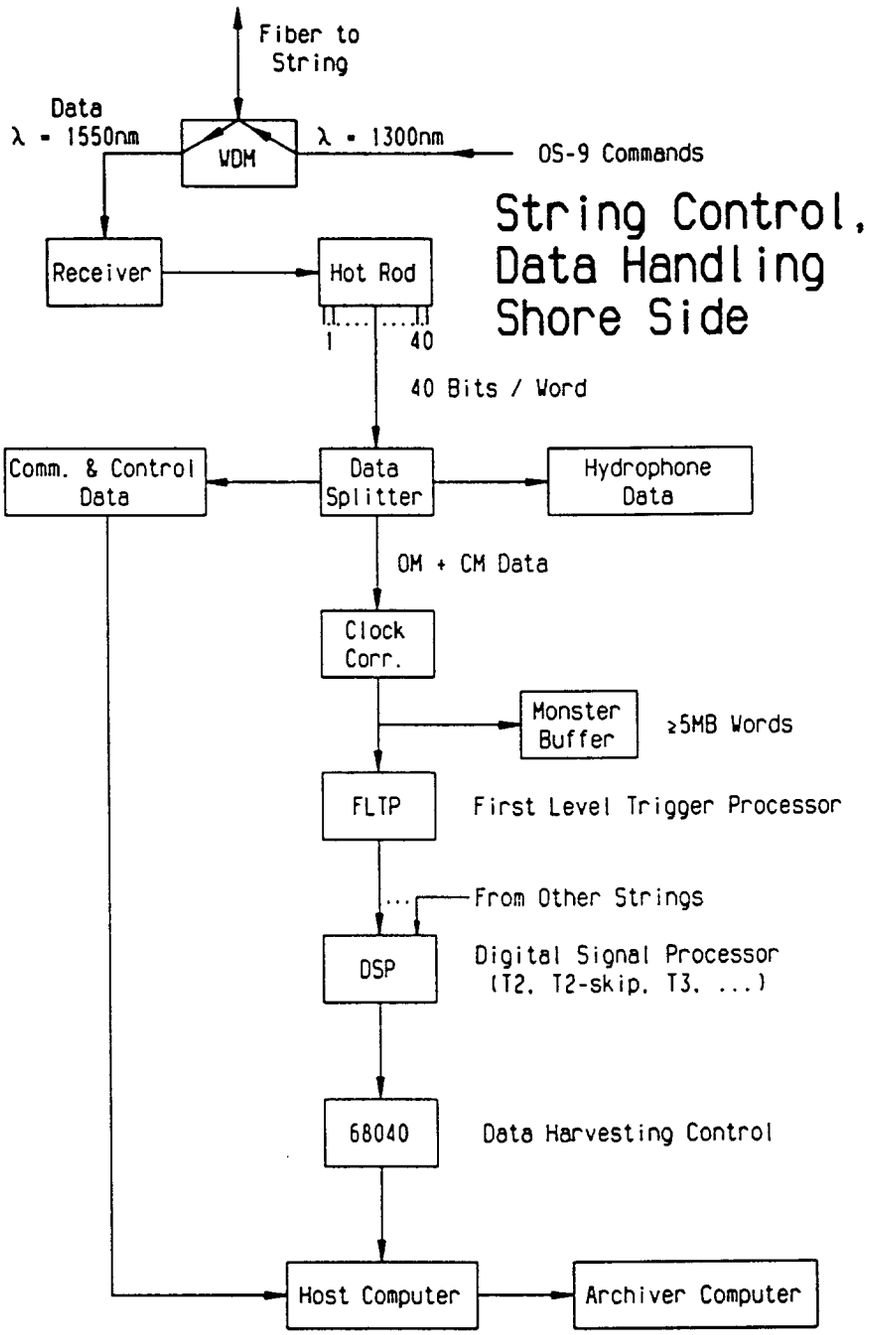

Figure 18: Block diagram of control, data flow and processing of a string and the full array at the shore side. For details see text.

operate the system.

5 Trigger Selection Criteria

In view of the high optical background level in the ocean discussed before a variety of trigger criteria have to be applied to filter out the desired events with the highest possible efficiency, yet discriminating most effectively against the background.

Fig. 18 illustrates the data flow as discussed earlier. After the clock correction which is necessary because of the independence of the string clocks the raw data are stored temporarily in the monster buffer and also sent to the first level trigger processor [25]. There simple one-string criteria such as nearest neighbor two-fold and three-fold coincidences, two out of three and three out of four coincidences with one miss, etc., occurring within a defined time window are required to pass the data on.

Subsequently the digital signal processor which gets the previously accepted data from all the strings searches for correlated events among all the strings over a larger time window. If the second level trigger criteria are successfully passed the event will proceed for trajectory reconstruction. If an event is of particular interest, data from a time interval before and after the occurrence of the particular event that did not pass one of the trigger criteria may now become of relevance and can be retrieved from the monster buffer for further correlation analysis.

6 Project Phase I: The TRIAD Configuration

6.1 General Comments.

A giant array such as the DUMAND Stage II octagon telescope cannot be completed all at once. The fabrication of a large number of units and modules requires many months. It is therefore sensible to test a first portion thoroughly before completion of the entire system. In view of this situation the principal funding agency requested that a first section of the full array be in satisfactory operation before giving the go-ahead for the remaining portion of the system. It was therefore decided to break up the project into two phases.

Phase I includes the completion of one third of the array together with the necessary infrastructure needed to operate the subsystem. This includes besides the

fabrication of three strings, the junction box and the 36 km twelve-fiber electro-optical cable, a first of its kind, also the cable laying operation, junction box deployment and installation on the ocean floor, and deployment and connection of the first three strings, before going into limited operation and attempting completion of the remaining six strings. The detector configuration of Phase I was named the TRIAD.

Obviously Phase I is well beyond the halfway mark of the entire budget since major development projects, such as the 1 GHz GaAs string digitizer chip, the 12-fiber electro-optical shore cable and junction box, the high speed data link from the array to shore, the command link from shore to the array, the sophisticated sonar system and unusual components, represented large financial engagements that, upon completion, are available for the remaining six strings at no or comparatively small extra costs. Nevertheless, in view of the great complexity of an entire string and of the finite possibility to have a hidden flaw in the system, the introduction of a go/no-go node in the project schedule is a sensible approach.

6.2 TRIAD Layout, Capabilities and Background.

The TRIAD configuration comprises the center string with the sonar and television systems, and two adjoining strings on the octagon circumference. In spite of the fact that the TRIAD is larger than any previous muon detector its usefulness as a neutrino telescope is at best very marginal. However, it will permit to fully test the command and data handling concept, the data acquisition and screening hardware and software, and the event reconstruction and background rejection software. Scientifically it will be a valuable tool to carry out high energy cosmic ray muon and atmospheric neutrino work.

The effective area of the TRIAD versus cosine of zenith angle is shown in Fig. 19 for muons of energy $\geq$ 100 GeV with an E^{-1} muon energy spectrum resulting from an E^{-2} neutrino spectrum. The median pointing error of reconstructed muon trajectories versus muon energy is given in Fig. 20. Details of the scientific merits and performance of the TRIAD configuration are described elsewhere [26]. We present therefore only the most relevant features for completeness.

The expected event rate for atmospheric and high energy neutrinos from active galactic nuclei are shown in Fig. 21. The total count of atmospheric neutrino induced events is expected to be about 40, and that of AGN induced events about 60 per year. The background rates due to the different sources are listed in Table 6.1.

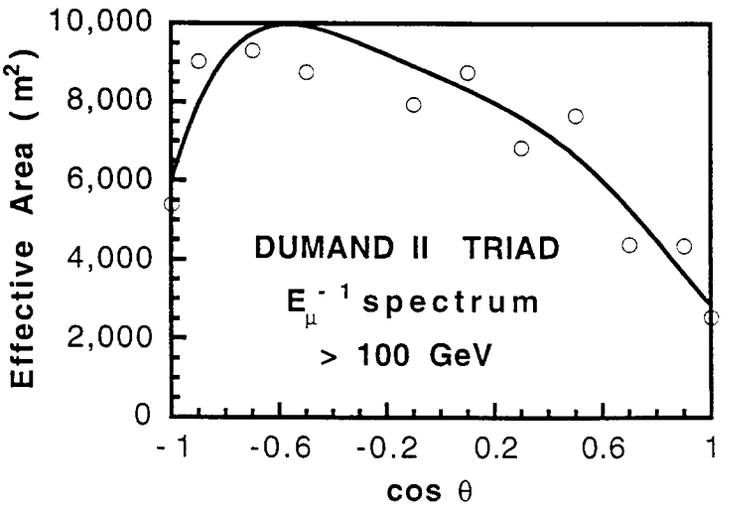

Figure 19: Effective area of the DUMAND II Triad versus cosine of the zenith angle, θ for a muon integral energy spectrum of the form E_μ^{-1} and energy $\geq 100GeV$.

7 Deployment and Installation of Junction Box, Shore Cable and Strings

Deployment of the junction box, laying of the shore cable, and deployment and connection of the first three strings to the junction box was initially scheduled for late October or early November 1993. Since junction box and cable form one unit and the strings separate units each, it was intended to break up the deployment of the TRIAD system into two or possibly three steps. This appeared to be necessary since few oceanographic vessels can accommodate so extremely bulky and heavy equipment as the forty by eight by eight foot reinforced cable tray and the junction box with a total weight of 55 tons, not including the giant winch and heavy gear that had to be installed for the deployment.

The 425 m long strings that are kept in large air conditioned containers to protect the phototubes from the intense sun while being stored on campus or on deck of the ship can, in principle, be deployed from a smaller vessel. They require, however, a robot or manned deep submersible for connection to the junction box, an operation that can be done in a third and separate step. Complex devices such as robots or manned submersibles usually have their own support vessel. Such a ship could also be used to deploy the strings if adequate space is available to store the string containers. Thus, a variety of scenarios can be envisaged.

Initially detailed plans for the deployment were worked out with the intention to use the Navy's *Independence*, a ship well suited for our purpose, late in October

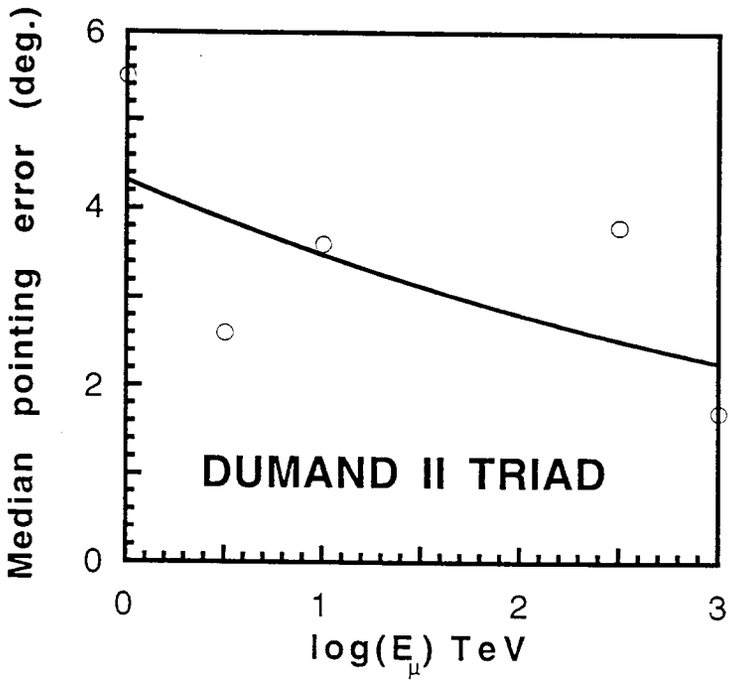

Figure 20: Median pointing error in degrees of the muon trajectory versus muon energy for the Triad detector.

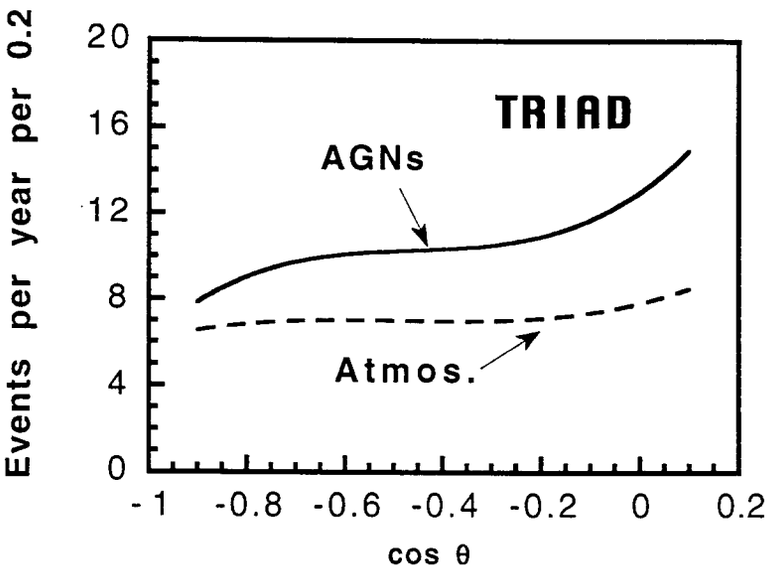

Figure 21: Number of events per year per 0.2 cosine(θ), where θ is the zenith angle, for neutrinos of atmospheric and AGN origin.

TABLE 6.1 : Background Sources and their Contributions to TRIAD.

Source	y^{-1} $(3^{o\ 2}$ pix$)^{-1}$
K^{40}	0.60
Cosmic ray muons	≤ 0.1
Cosmic ray multi-muons	
Atmospheric neutrinos	0.03
Total	0.73
Enclosed volume	$2.5{\cdot}10^5$ m^3

and into November. However, it became known by early fall that for technical and operational reasons no robot or manned deep submersible would be available for the target date to connect the strings to the junction box, leaving the TRIAD incomplete and inoperative. It was therefore decided to attach string 1 directly to the junction box and to deploy it together with the latter and the shore cable in one complex operation. The particular deployment scheme that was now necessary to prevent entanglement of string and shore cable is illustrated in Fig. 22.

The new and significantly more complex deployment operation that had to be performed now required careful preparation. In September 1993 a trial deployment with the combined configuration of string 1, junction box and a test cable was carried out from the University of Hawaii's own research vessel *Moana Wave*, a relatively small ship that could not accommodate the shore cable and did not have the equipment to hold a definite position at sea for any length of time. Nevertheless, this exercise was of great value as it showed where problems could arise.

By the end of October it became clear that not only was there no robot or equivalent device available during the months to follow, but also the Navy's *Independence* would not be available at that time because of other commitments. Fortunately, the *Thomas G. Thompson*, one of the most modern oceanographic research vessel presently in service, could be contracted in its place from November 26 until December 18.

The T.G. Thompson which measures almost 100 m in length with large work areas, could easily accommodate all our heavy equipment, including the 55 ton cable

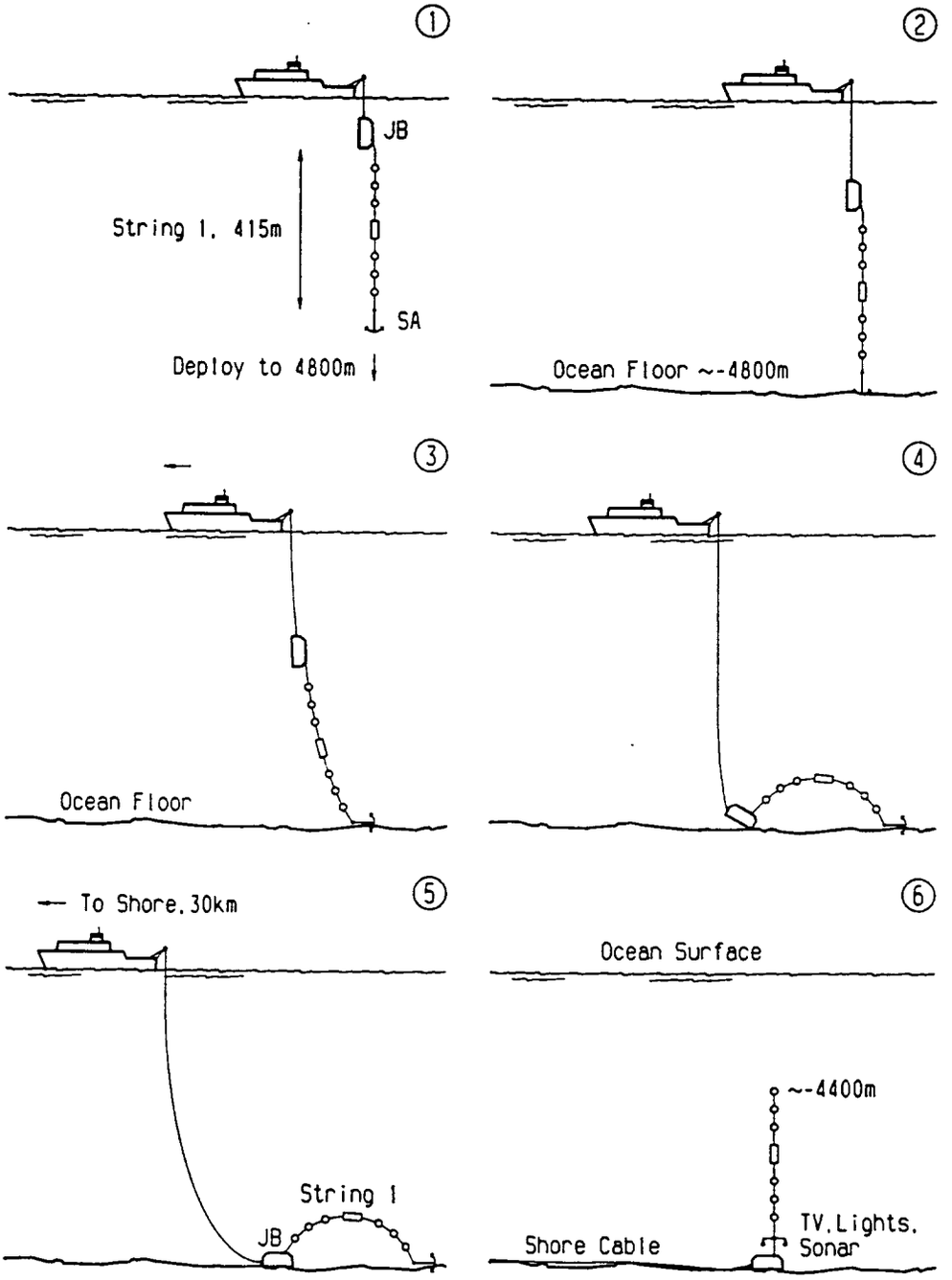

Figure 22: Deployment principle for string 1, junction box and subsequent laying of the shore cable. The 6 drawings show the relevant phases of the operation. SA is the sacrificial anchor.

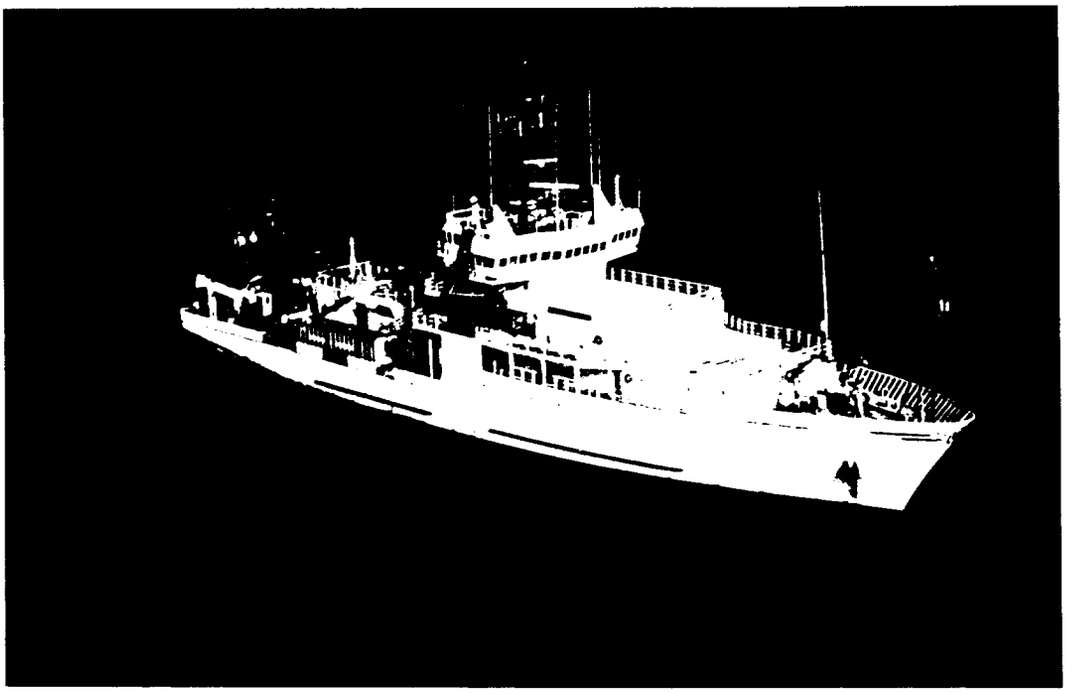

Figure 23: The research vessel T. G. Thompson, operated by the University of Washington, Seattle, at the DUMAND site during deployment of the junction box and string 1 of the TRIAD (December 14, 1993).

tray with the 35 km of electro-optical shore cable, the giant winch that was needed to deploy the 2500 kg heavy junction box together with the center string and shore cable, and the remaining two string containers. Deployment of all parts of the TRIAD appeared now possible. Unfortunately installation of all the special gear on board the ship was more difficult than anticipated and major problems with the big winch required extensive tests with dummy loads at Snug Harbor in Honolulu that consumed much valuable time. In addition bad weather and other technical problems prevented the ship from sailing to the site until December 9, 1993.

The combined deployment of string 1, junction box and shore cable, including cable laying, was one of the most complex and precise operation of its kind ever done at sea, and one of the most complex systems so far placed at the ocean floor at this depth. Lowering and deployment of string 1 and the junction box required about 10.5 hours until the junction box was properly placed at the correct position. Fig. 23 shows the T. G. Thompson during deployment at the DUMAND site and Fig. 24 a scene of the deployment procedure of string 1.

During deployment the system was continuously powered and monitored. However, to avoid possible damage to the photocathodes due to background light, the

Figure 24: Deployment of detector module from the T. G. Thompson research vessel at the DUMAND site. Portion of the junction box is visible on the left.

high voltage of the phototubes was turned on only after the string had reached a depth of 1000 m. About three hours after taking string 1 into operation module number 11 began to produce errors while the rest appeared to be in working order. After about 10 hours of data taking string 1 ceases to operate. A total of approximately 3 Gbyte of data was acquired during the entire deployment phase by the monster buffer. The contents of the latter was dumped periodically onto a tape. Analysis of the data is now in progress.

The cable laying operation took about 36 hours and was a full success. It was not a trivial task since a carefully chosen route that was previously selected on the basis of detailed surveys had to be followed closely, to imposed the least inherent risks for the cable. Since the laying of the cable was part of step 1 it had to be completed before any further step could be initiated. Any interruption could have been fatal for the delicate shore cable. Recovery of the cable with the junction box attached would have been without major problems as long as the cable was outside the topographically difficult slope to the shore. Once placed in the trenches and canyons the cable could almost certainly not be recovered without being damaged.

After passing the shore cable trough the 200 m long conduit and connecting it to the shore station, tests revealed that electrically the junction box was fully

operational. Of the twelve fibers in the cable eleven are in perfect working order; one fiber is broken at kilometer 20 from the shore. This location is not at a cable splice but in the middle of a cable section and is thought to be a manufacturing defect. The availability of only eleven fibers is of no concern since only ten are needed, the remaining were intended to be spares.

Subsequently extensive tests were carried out from the shore station with the sonar system at the junction box and in the lower portion of the string that was fully operational. Likewise one of the two television system with its floodlights was in perfect working order and delivered excellent pictures of the junction box and the lower portion of the string. The other of-the-shelf deep sea television camera failed shortly after the beginning of deployment. That the failure occurred in the camera could easily be verified by switching the working camera from one transmission channel to the other.

Since the sonar and television systems represent an autonomous subsystem with its own controller, it was not affected by the breakdown of the command and data links of string 1. Failure of the latter prevented the command to release the sacrificial three-ton anchor at the top end of the string from being executed, thus leaving the string in an arched position, as shown in Fig. 22-5.

8 Recovery and Inspection of String 1

Since the sacrificial anchor could not be released by command, the string could not be recovered until the magnesium time fuse, which is activated by corrosion in ocean water, would open and release the top of the string. This was expected to take place about three weeks after deployment. It did occur in fact in the middle of January when the television monitor revealed that the string was now in its normal vertical operating position (Fig. 22-6).

On January 27, 1994 a crew of twelve, including eight members of the DUMAND collaboration, reached the site at 3:20 am on board the 120-foot work boat Noho'Loa. The release command was given at 4:40 am and the release of the string was immediately observed by the shore station. The string surfaced 63 minutes later and was recovered by the crew and brought back to Honolulu.

A first inspection revealed that module number 11 had suffered a leak. This was the first time in the long history of deployment and pressure tests, including the short prototype experiment with its many deep deployments and recoveries, that a leak had developed in an optical module. This by itself would have been of no major concern for the successful operation of the string.

However, it was also discovered that the string center controller held about 4.5 liters of sea water in its net volume of roughly 60 liters. This was the cause for

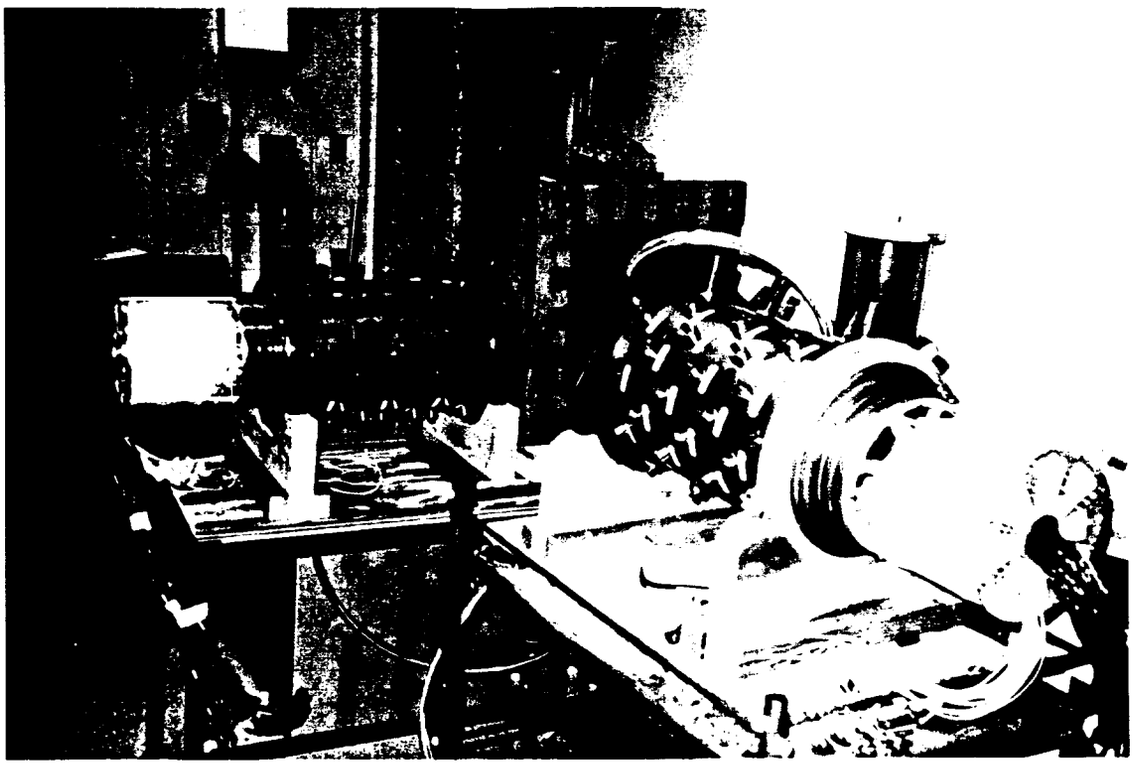

Figure 25: The two large tubes, called "porcupines" because of the many penetrators on their circumference, are made of 1-inch thick titanium and hold a total of almost 60 optical and electrical penetrators. The right hand portion of the unit in the foreground holds the optical fibers (white portion), and in the center are the black electrical cables that both connect to the controller electronics (not shown).

the string failure and also explains the necessity to re-boot the system from time to time during deployment. From that behavior one is lead to the tentative conclusion that a leak must have developed very likely at an early stage of deployment, in rather shallow water, and that it disappeared later on when the surrounding pressure increased.

Careful inspection and analysis is now under way to determine the actual cause for the leak in the string controller. Since the so-called porcupine portion of the controller housing (Fig. 25) holds a total of almost 60 penetrators in its one inch thick titanium housing, the string controller is a very delicate part. However, all penetrators, optical and electrical, had been tested individually to pressures up to 10.000 psi ($\sim$ 680 atm.), and the entire controller housing after installation of the penetrators. It therefore seems to be more likely that a leak developed at the endcap which had to be removed to insert the system after testing. A tiny leak at this location could be sealed off under very high pressure, thus permitting only a

very limited, yet fatal quantity of water, to enter the control system.

9 Concluding Remarks

The DUMAND Collaboration plans to replace the destroyed string controller and the flooded module, and will prepare string 1 together with the two other completed strings for deployment as soon as possible. Since all technological developments are completed, progress is a matter of fabrication effort, which depends essentially on the availability of funds.

10 Acknowledgements

The DUMAND Collaboration is grateful to the following organizations and funding agencies for supporting the project: Bundesministerium für Forschung und Technologie (BMFT), Germany; Federal State of Schleswig - Holstein, Germany; Japanese Science Foundation Mombusho; Japan Society for the Promotion of Science; Swiss National Science Foundation; U.S. Department of Energy; U.S. National Science Foundation; Wolfermann - Nägeli Stiftung, Kilchberg, Switzerland.

References

[1] P.K.F. Grieder: "A New Window on the Universe". Europhysics News, 23, Nr. 9, p. 167-169 (1992).

[2] P. Bosetti, P.K.F. Grieder, W. Gajewski, W. Kropp, L. Price, F. Reines, H. Sobel, B. Barish, J. Elliott, J. Babson, R. Becker-Szendy, J.G. Learned, S. Matsuno, D. O'Connor, A. Roberts, V.J. Stenger, V.Z. Peterson, G. Wilkins, O.C. Allkofer, P. Koske, M. Preischel, J. Rathlev, T. Kitamura, H. Bradner, K. Mitsui, Y. Ohashi, A. Okada, J. Clem, C.E. Roos, M. Webster, U. Camerini, M. Jaworski, R. March, and R. Morse. DUMAND II. Proposal to construct a deep ocean laboratory for the study of high energy neutrino astrophysics and particle physics. University of Hawaii Publication, HDC-2-88, p. 1-155 (1988).

[3] J. Babson, B. Barish, R. Becker-Szendy, H. Bradner, R. Cady, J. Clem, S. Dye, J. Gaidos, P. Gorham, P.K.F. Grieder, T. Kitamura, W. Kropp, J.G. Learned, S. Matsuno, R. March, K. Mitsui, D. O'Connor, Y. Ohashi, A. Okada, V. Peterson, L. Price, F. Reines, A. Roberts, C. Roos, H. Sobel, V.J. Stenger, M. Webster, C. Wilson: Cosmic Ray Muons in the Deep Ocean. Phys. Rev. D 42, p. 3613-3620 (1990).

[4] J.G. Learned: High Energy Neutrino Astronomy and Astrophysics: An Outlook into the Future, in COSMIC RAYS 92 - Astrophysical, High Energy and Heliospheric Processes. Ed. P.K.F. Grieder, Nucl. Phys. B (Proc. Suppl.) 33A,B (1993), May 1993.

[5] P.K.F. Grieder: "The DUMAND Stage II Deep Underwater Muon and Neutrino Telescope". Invited LectureProceedings of the 6th Internat. Symposium on Very High Energy Cosmic Ray Interactions, Tarbes, France (1990). Edited by J.N. Capdevielle and P. Gabinski, Université de Bordeaux I, p. 117-167 (1991).

[6] V. Stenger: Neutrino Oscillations in the Sea. Proceedings of the 2nd Nestor International Workshop, October 1992, Pylos, Greece, L. Resvanis ed., p. 110 (1993).

[7] J.G. Learned for the DUMAND Collaboration: C.M. Alexander, T. Aoki, U. Berson, P. Bosetti, J. Bolesta, P.E. Boynton, H. Bradner, U. Camerini, S.T. Dye, M. Fukawa, E. Gergin, P.W. Gorham, G. Grajew, P.K.F. Grieder, W. Grogan, H. Hanada, D. Harris, T. Hayashino, E. Hazen, M. Ito, M. Jaworksi, M. Jenko, H. Kawamoto, T. Kitamura, K. Kobayakawa, S. Kondo, P. Koske, J.G. Learned, J.J. Lord, R. Lord, T. Lozic, R. March, T. Matsumoto, S. Matsuno, A. Mavretic, L. McCourry, M. Mignard, K. Miller, P. Minkowski, R. Mitiguy, K. Mitsui, S. Narita, D. Nicklaus, Y. Ohashi, A. Okada, D. Orlov, V.Z. Peterson, A. Roberts, V.J. Stenger, T. Takayama, S. Tanaka, S. Uehara, C. Wiebusch, G. Wilkins, M. Webster, R.J. Wilkes, G. Wurm, O. Watanabe, A. Yamaguchi, I. Yamamoto, K.K. Young: "Acoustical Neutrino Detection in DUMAND". Proceedings of the XXIII. Internat. Cosmic Ray Conf., Calgary, Canada, 4, p. 538 (1993).

[8] V.J. Stenger: Optimizing Deep Underwater Neutrino Detectors. Proceedings of the 2nd Nestor International Workshop, October 1992, Pylos, Greece, L. Resvanis ed., p. 101 (1993).

[9] J.R.V. Zaneveld: Optical Properties of the Keahole-DUMAND Site. Proceedings of the 1980 International DUMAND Symposium, Honolulu, Hawaii, 1, p. 1 (1980).

[10] T. Aoki, T. Kitamura, S. Matsuno, K. Mitsui, Y. Ohashi, A. Okada, D.R. Cady, J.G. Learned, D. O'Connor, M. McMurdo, R. Mitiguy, M. Webster, C. Wilson,

and P. Grieder: Background Light Measurements at the DUMAND Site. Proc. 19th Internat. Cosmic Ray Conf., La Jolla, CA, 8, p. 53-56 (1985).

[11] T. Aoki, T. Kitamura, S. Matsuno, K. Mitsui, Y. Ohashi, A. Okada, D.R. Cady, J.G. Learned, P. O'Connor, M. McMurdo, R. Mitiguy, P. Grieder, M. Webster, and C. Wilson: Background Light Measurements in the Deep Ocean. Nuovo Cimento 9C, p. 642-652 (1986).

[12] H.G. Berns, J. George, R. Lord, J.J. Lord, L. McCourry, R.J. Wilkes, and K.K. Young for the DUMAND Collaboration: C.M. Alexander, T. Aoki, H.G. Berns, U. Berson, P. Bosetti, J. Bolesta, P.E. Boynton, H. Bradner, U. Camerini, S.T. Dye, M. Fukawa, E. Gergin, P.W. Gorham, G. Grajew, P.K.F. Grieder, W. Grogan, H. Hanada, D. Harris, T. Hayashino, E. Hazen, M. Ito, M. Jaworksi, M. Jenko, H. Kawamoto, T. Kitamura, K. Kobayakawa, S. Kondo, P. Koske, J.G. Learned, J.J. Lord, R. Lord, T. Lozic, R. March, T. Matsumoto, S. Matsuno, A. Mavretic, L. McCourry, M. Mignard, K. Miller, P. Minkowski, R. Mitiguy, K. Mitsui, S. Narita, D. Nicklaus, K.M. O'Brien, Y. Ohashi, A. Okada, D. Orlov, V.Z. Peterson, A. Roberts, V.J. Stenger, T. Takayama, S. Tanaka, S. Uehara, C. Wiebusch, G. Wilkins, M. Webster, R.J. Wilkes, G. Wurm, O. Watanabe, A. Yamaguchi, I. Yamamoto, K.K. Young: " Acoustical Locating System for DUMAND II". Proceedings of the XXIII. Internat. Cosmic Ray Conf., Calgary, Canada, 4, p. 542 (1993).

[13] G. van Aller, S-O Flyckt, P. Linders and P. Bosetti: "A Smart 35 cm Diameter Photomultiplier". Helvetica Physica Acta, 59, p. 1119 (1986).

[14] A. Okada and K.M. O'Brien for the DUMAND Collaboration: C.M. Alexander, T. Aoki, U. Berson, P. Bosetti, J. Bolesta, P.E. Boynton, H. Bradner, U. Camerini, S.T. Dye, M. Fukawa, E. Gergin, P.W. Gorham, G. Grajew, P.K.F. Grieder, W. Grogan, H. Hanada, D. Harris, T. Hayashino, E. Hazen, M. Ito, M. Jaworksi, M. Jenko, H. Kawamoto, T. Kitamura, K. Kobayakawa, S. Kondo, P. Koske, J.G. Learned, J.J. Lord, R. Lord, T. Lozic, R. March, T. Matsumoto, S. Matsuno, A. Mavretic, L. McCourry, M. Mignard, K. Miller, P. Minkowski, R. Mitiguy, K. Mitsui, S. Narita, D. Nicklaus, K.M. O'Brien, Y. Ohashi, A. Okada, D. Orlov, V.Z. Peterson, A. Roberts, V.J. Stenger, T. Takayama, S. Tanaka, S. Uehara, C. Wiebusch, G. Wilkins, M. Webster, R.J. Wilkes, G. Wurm, O. Watanabe, A. Yamaguchi, I. Yamamoto, K.K. Young: "Estimate of Downgoing Atmospheric Muon Background Events in DUMAND II". Proceedings of the XXIII. Internat. Cosmic Ray Conf., Calgary, Canada, 4, p. 523 (1993).

[15] V.J. Stenger: High Energy Neutrino Astrophysics. Proceedings of the 2nd Nestor International Workshop, October 1992, Pylos, Greece, L. Resvanis ed., p. 79 (1993).

[16] F.W. Stecker, C. Done, M.H. Salamon, and P. Sommers: Phys. Rev. Lett. 66, p. 2697 (1991).

[17] A. Okada: Proceedings of the Workshop on High energy Neutrino Astrophysics, University of Hawaii, 1992, p. 277. Ed. V.J. Stenger, J.G. Learned, S. Pakvasa and X. Tata. World Scientific, Singapore (1992).

[18] A. Okada and J. Hauptman for the DUMAND Collaboration: C.M. Alexander, T. Aoki, U. Berson, P. Bosetti, J. Bolesta, P.E. Boynton, H. Bradner, U. Camerini, S.T. Dye, M. Fukawa, E. Gergin, P.W. Gorham, G. Grajew, P.K.F. Grieder, W. Grogan, H. Hanada, D. Harris, T. Hayashino, E. Hazen, M. Ito, M. Jaworksi, M. Jenko, H. Kawamoto, T. Kitamura, K. Kobayakawa, S. Kondo, P. Koske, J.G. Learned, J.J. Lord, R. Lord, T. Lozic, R. March, T. Matsumoto, S. Matsuno, A. Mavretic, L. McCourry, M. Mignard, K. Miller, P. Minkowski, R. Mitiguy, K. Mitsui, S. Narita, D. Nicklaus, Y. Ohashi, A. Okada, D. Orlov, V.Z. Peterson, A. Roberts, V.J. Stenger, T. Takayama, S. Tanaka, S. Uehara, C. Wiebusch, G. Wilkins, M. Webster, R.J. Wilkes, G. Wurm, O. Watanabe, A. Yamaguchi, I. Yamamoto, K.K. Young: "On the Detection of Ultrahigh Energy Cascade Showers with DUMAND II". Proceedings of the XXIII. Internat. Cosmic Ray Conf., Calgary, Canada, 4, p. 772 (1993).

[19] P.L. Biermann: Neutrino Spectra from Active Galactic Nuclei - The Disk Component. Proceedings of the Workshop on High energy Neutrino Astrophysics, University of Hawaii, 1992, p. 86. Ed. V.J. Stenger, J.G. Learned, S. Pakvasa and X. Tata. World Scientific, Singapore (1992).

[20] V.J. Stenger: Atmospheric Neutrino Oscillations with DUMAND. University of Hawaii, DUMAND-11-93 (1993).

[21] S. Matsuno, J. Babson, J.G. Learned, D. O'Connor, P.K. Grieder, K. Mitsui, Y. Ohashi, A. Okada, J. Clem, M. Webster, and C. Wilson: Single photon light detector for deep ocean applications. Nuclear Instruments and Methods, A276, pp. 359-366 (1989).

[22] The DUMAND Collaboration: C.M. Alexander, T. Aoki, U. Berson, P. Bosetti, J. Bolesta, P.E. Boynton, H. Bradner, U. Camerini, S.T. Dye, M. Fukawa, E. Gergin, P.W. Gorham, G. Grajew, P.K.F. Grieder, W. Grogan, H. Hanada, D. Harris, T. Hayashino, E. Hazen, M. Ito, M. Jaworksi, M. Jenko, H. Kawamoto, T. Kitamura, K. Kobayakawa, S. Kondo, P. Koske, J.G. Learned, J.J. Lord, R. Lord, T. Lozic, R. March, T. Matsumoto, S. Matsuno, A. Mavretic, L. McCourry, M. Mignard, K. Miller, P. Minkowski, R. Mitiguy, K. Mitsui, S. Narita, D. Nicklaus, Y. Ohashi, A. Okada, D. Orlov, V.Z. Peterson, A. Roberts, V.J. Stenger, T. Takayama, S. Tanaka, S. Uehara, C. Wiebusch, G. Wilkins, M. Webster, R.J. Wilkes, G. Wurm, O. Watanabe, A. Yamaguchi, I. Yamamoto, K.K. Young: "Optical Module for DUMAND II - Japanese Version". Proceedings of the XXIII. Internat. Cosmic Ray Conf., Calgary, Canada, 4, p. 546 (1993).

[23] P.C. Bosetti for the DUMAND Collaboration: C.M. Alexander, T. Aoki, U. Berson, P. Bosetti, J. Bolesta, P.E. Boynton, H. Bradner, U. Camerini, S.T. Dye, M. Fukawa, E. Gergin, P.W. Gorham, G. Grajew, P.K.F. Grieder, W. Grogan, H. Hanada, D. Harris, T. Hayashino, E. Hazen, M. Ito, M. Jaworksi, M. Jenko, H. Kawamoto, T. Kitamura, K. Kobayakawa, S. Kondo, P. Koske, J.G. Learned, J.J. Lord, R. Lord, T. Lozic, R. March, T. Matsumoto, S. Matsuno, A. Mavretic, L. McCourry, M. Mignard, K. Miller, P. Minkowski, R. Mitiguy, K. Mitsui, S. Narita, D. Nicklaus, Y. Ohashi, A. Okada, D. Orlov, V.Z. Peterson, A. Roberts, V.J. Stenger, T. Takayama, S. Tanaka, S. Uehara, C. Wiebusch, G. Wilkins, M. Webster, R.J. Wilkes, G. Wurm, O. Watanabe, A. Yamaguchi, I. Yamamoto, K.K. Young: "An Optical Sensor for DUMAND II - European Version". Proceedings of the XXIII. Internat. Cosmic Ray Conf., Calgary, Canada, 4, p. 534 (1993).

[24] E. Hazen for the DUMAND Collaboration: C.M. Alexander, T. Aoki, U. Berson, P. Bosetti, J. Bolesta, P.E. Boynton, H. Bradner, U. Camerini, S.T. Dye, M. Fukawa, E. Gergin, P.W. Gorham, G. Grajew, P.K.F. Grieder, W. Grogan, H. Hanada, D. Harris, T. Hayashino, E. Hazen, M. Ito, M. Jaworksi, M. Jenko, H. Kawamoto, T. Kitamura, K. Kobayakawa, S. Kondo, P. Koske, J.G. Learned, J.J. Lord, R. Lord, T. Lozic, R. March, T. Matsumoto, S. Matsuno, A. Mavretic, L. McCourry, M. Mignard, K. Miller, P. Minkowski, R. Mitiguy, K. Mitsui, S. Narita, D. Nicklaus, Y. Ohashi, A. Okada, D. Orlov, V.Z. Peterson, A. Roberts, V.J. Stenger, T. Takayama, S. Tanaka, S. Uehara, C. Wiebusch, G. Wilkins, M. Webster, R.J. Wilkes, G. Wurm, O. Watanabe, A. Yamaguchi, I. Yamamoto, K.K. Young: "The DUMAND II Digitizer". Proceedings of the XXIII. Internat. Cosmic Ray Conf., Calgary, Canada, 4, p. 768 (1993).

[25] U. Camerini for the DUMAND Collaboration: C.M. Alexander, T. Aoki, U. Berson, P. Bosetti, J. Bolesta, P.E. Boynton, H. Bradner, U. Camerini, S.T. Dye, M. Fukawa, E. Gergin, P.W. Gorham, G. Grajew, P.K.F. Grieder, W. Grogan, H. Hanada, D. Harris, T. Hayashino, E. Hazen, M. Ito, M. Jaworksi, M. Jenko, H. Kawamoto, T. Kitamura, K. Kobayakawa, S. Kondo, P. Koske, J.G. Learned, J.J. Lord, R. Lord, T. Lozic, R. March, T. Matsumoto, S. Matsuno, A. Mavretic, L. McCourry, M. Mignard, K. Miller, P. Minkowski, R. Mitiguy, K. Mitsui, S. Narita, D. Nicklaus, Y. Ohashi, A. Okada, D. Orlov, V.Z. Peterson, A. Roberts, V.J. Stenger, T. Takayama, S. Tanaka, S. Uehara, C. Wiebusch, G. Wilkins, M. Webster, R.J. Wilkes, G. Wurm, O. Watanabe, A. Yamaguchi, I. Yamamoto, K.K. Young: "Trigger Strategies and Processing for DUMAND". Proceedings of the XXIII. Internat. Cosmic Ray Conf., Calgary, Canada, 4, p. 530 (1993).

[26] V.J. Stenger for the DUMAND Collaboration: C.M. Alexander, T. Aoki, U. Berson, P. Bosetti, J. Bolesta, P.E. Boynton, H. Bradner, U. Camerini, S.T. Dye, M. Fukawa, E. Gergin, P.W. Gorham, G. Grajew, P.K.F. Grieder, W. Grogan, H. Hanada, D. Harris, T. Hayashino, E. Hazen, M. Ito, M. Jaworksi, M.

Jenko, H. Kawamoto, T. Kitamura, K. Kobayakawa, S. Kondo, P. Koske, J.G. Learned, J.J. Lord, R. Lord, T. Lozic, R. March, T. Matsumoto, S. Matsuno, A. Mavretic, L. McCourry, M. Mignard, K. Miller, P. Minkowski, R. Mitiguy, K. Mitsui, S. Narita, D. Nicklaus, K.M. O'Brien, Y. Ohashi, A. Okada, D. Orlov, V.Z. Peterson, A. Roberts, V.J. Stenger, T. Takayama, S. Tanaka, S. Uehara, C. Wiebusch, G. Wilkins, M. Webster, R.J. Wilkes, G. Wurm, O. Watanabe, A. Yamaguchi, I. Yamamoto, K.K. Young: "Capabilities of the DUMAND II Pase I - 3 String Array". Proceedings of the XXIII. Internat. Cosmic Ray Conf., Calgary, Canada, 4, p. 527 (1993).

The DUMAND Collaboration

W . Anderson [16], T. Aoki [10] (E) [4], H. G. Berns [14] (E), U. Berson [13], P. Bosetti [13], J. Bolesta [3], P.E. Boynton [14], H. Bradner [8], U. Braun [13], U. Camerini [15], R. Clark [17]; S.T. Dye [2], M. Fukawa [11], J. George [14], E. Gergin [2] (E), P.W. Gorham [3], P.K.F. Grieder [1], W. Grogan [15] (E), H. Hanada [9] (E), D. Harris [3] (E), J. Hauptman [16], T. Hayashino [9], E. Hazen [2] (E), A. Iwasaki [9], M. Jaworksi [15] (E), M. Jenko [2] (E), A. Kibayashi [3], T. Kitamura [6], K. Kobayakawa [5], S. Kondo [3], P. Koske [4], J.G. Learned [3], C. Ley [13], J.J. Lord [14], R. Lord [14] (E), T. Lozic [2] (E), R. March [15], T. Matsumoto [9], S. Matsuno [3], A. Mavretic [2] (E), L. McCourry [14] (E), M. Mignard [3] (E), K. Miller [12], P. Minkowski [1], R. Mitiguy [3] (E), K. Mitsui [10], S. Narita [9], T. Narita [15], D. Nicklaus [15] (E), K. O'Brien [16], Y. Ohashi [10], A. Okada [10], D. Orlov [2] (E), V.Z. Peterson [3], A. Roberts [3], M. Sakuda [11], V.J. Stenger [3], R. Svoboda [17]; T. Takayama [9] (E), D. Takemori [3], S. Tanaka [18], S. Uehara [11], C.H. Wiebusch [13], G. Wilkins [3] (E), M. Webster [12], R.J. Wilkes [14], G. Wurm [13], A. Yamaguchi [9], I. Yamamoto [7] (E), and K.K. Young [14]

[1] University of Bern, Switzerland
[2] Boston University, USA
[3] University of Hawaii, USA
[4] University of Kiel, Germany
[5] Kobe University, Japan
[6] Kinki University, Japan
[7] Okayama Science University, Japan
[8] Scripps Institution of Oceanography, USA
[9] Tohoku University, Japan
[10] ICRR, University of Tokyo, Japan
[11] KEK, Tsukuba, Japan
[12] Vanderbilt University, USA
[13] Vijlen Institute for Physics, Netherlands
[14] University of Washington, USA
[15] University of Wisconsin, USA
[16] Iowa St. University, USA
[17] Louisiana State University, USA
[18] Hirosaki University, Japan

[4](E) engineer